Received: 29 October 2021 | Revised: 16 February 2022 | Accepted: 21 February 2022 | Published on: 4 March 2022

DOI: 10.1002/joc.7587

RESEARCH ARTICLE

International Journal of Climatology RMetS

Record summers in Europe: Variations in drought and heavy precipitation during 1901–2018

Stephanie Hänsel[1,2] | **Andreas Hoy**[1] | **Christoph Brendel**[2] | **Maurizio Maugeri**[3]

[1]Interdisciplinary Environmental Research Center, TU Bergakademie Freiberg, Freiberg, Germany

[2]Section Climate and Environment, Deutscher Wetterdienst, Offenbach am Main, Germany

[3]Department of Environmental Science and Policy, Università degli Studi di Milano, Milan, Italy

Correspondence
Stephanie Hänsel, Deutscher Wetterdienst, Section Climate and Environment, Frankfurter Str. 135, 63067 Offenbach am Main, Germany.
Email: stephanie.haensel@dwd.de

Abstract

During the last 20 years some very hot and dry summers affected Europe, resulting in regionally record-breaking high temperature or low precipitation values. Long-term changes of such extremely hot and dry summers are of great relevance for our society, as they are connected with manifold negative impacts on human society, natural ecosystems, and diverse economic sectors. Long-term variations in drought and five record drought summer half years are studied based on 63 stations across Europe with high-quality precipitation and temperature time series spanning the period 1901–2018. Eight drought indices are deployed to analyse drought intensity, frequency, and duration; four of them purely precipitation-based and four integrating potential evapotranspiration in the computation. Additionally, three heavy precipitation indices and simultaneous increases in drought and heavy precipitation are studied. The five driest summer half years over Europe are identified (1947, 2018, 2003, 1921, and 1911). They are analysed by aggregating eight drought indices into the aggregated drought evaluation index (ADE) for five subregions. The ADE shows increasing summer drought conditions over most of Europe, except for some stations in northern Europe. The increase in drought conditions during the warm part of the year is particularly pronounced for indices integrating evapotranspiration in their definition. At the same time, the intensity of heavy precipitation events shows a positive trend, as well as an increased contribution to total precipitation. Several stations in central Europe show simultaneously increasing drought conditions and increasing heavy precipitation events. This increases the risks connected with precipitation extremes.

KEYWORDS

climate indices, climate variability and change, dry periods, mRAI, WBAI

1 | INTRODUCTION

Several recent drought events demonstrated the challenges droughts pose for economic activities in Europe. The latest examples of severe meteorological drought events in Europe were the summers of 2003 (Fink *et al.*, 2004; Rebetez *et al.*, 2006), 2010 (Barriopedro *et al.*, 2011), 2015 (Hoy *et al.*, 2017; Ionita *et al.*, 2017), and 2018 (Masante

et al., 2018; Peters *et al.*, 2020; Zscheischler and Fischer, 2020). Nonetheless, such summer droughts in Europe are not a new phenomenon of the beginning of the 21th century. Already the 1940s and the 1950s have in fact experienced several significant drought events (Briffa *et al.*, 1994; Lloyd-Hughes and Saunders, 2002; Van der Schrier *et al.*, 2006; Spinoni *et al.*, 2015a). For instance, the extraordinary drought event during the summer half year of 1947 that affected central Europe had wide ranging socio-economic consequences (Brazdil *et al.*, 2016). Extreme summer drought events and episodes also occurred in earlier centuries such as in 1540 (Wetter *et al.*, 2014; Pfister, 2018) or the decade 1531–1540 (Brázdil *et al.*, 2020).

Such meteorological droughts often propagate through all parts of the hydrological cycle and develop into agricultural (soil moisture) and hydrological droughts. Respective drought impacts on different systems can thus be observed considerably longer as indicated by the precipitation deficits measured by meteorological indices. Reported impacts connected with these droughts include decreased streamflow or groundwater levels (Koehler *et al.*, 2007; Kohn *et al.*, 2014; Laaha *et al.*, 2017), adverse effects on agriculture and forestry (Ciais *et al.*, 2005; Hlavinka *et al.*, 2009; Allen *et al.*, 2010; Buras *et al.*, 2020; Schuldt *et al.*, 2020), and limitations in the energy production (De Bono *et al.*, 2004; Fink *et al.*, 2004). In the long run, persistent lower-than-average precipitation conditions may even lead to soil degradation and desertification (Nicholson *et al.*, 1998; Hueso *et al.*, 2012).

Besides these summer drought events, there is also concern about heavy precipitation events and connected flash floods and river floods. These are often connected with devastating impacts on society and the economy with casualties and high costs due to direct infrastructure and indirect socio-economic damages. Such events include the 2002 flood along the Elbe and Odra rivers and their tributaries (Ulbrich *et al.*, 2003; Kundzewicz *et al.*, 2005; Thieken *et al.*, 2005; Socher and Bohme-Korn, 2008), the 2013 flood along the Danube and Elbe rivers (Belz *et al.*, 2014; Merz *et al.*, 2014; Schröter *et al.*, 2015; Thieken *et al.*, 2016), the exceptional sequence of thunderstorms and connected flash-flood events, for example, in Braunsbach/Germany in 2016 (Piper *et al.*, 2016; Bronstert *et al.*, 2017; 2018), as well as the flooding events in July 2021 in western Europe (Junghänel *et al.*, 2021; Kreienkamp *et al.*, 2021), among many others.

The rising average global surface temperature and the related increase in water pressure deficit (Wang *et al.*, 2012; Yuan *et al.*, 2019; Grossiord *et al.*, 2020) increasingly impact the observed severity of drought events, especially during the warmest part of the year (Vicente-Serrano *et al.*, 2014). Extremely high temperatures or long-lasting heatwaves often accompanied recent drought events (Rebetez *et al.*, 2006; Graczyk and Kundzewicz, 2014; Hoy *et al.*, 2017; Sedlmeier *et al.*, 2018). Such droughts under warmer temperatures are sometimes referred to as "global-change-type droughts" (Breshears *et al.*, 2005; Adams *et al.*, 2009; Eamus *et al.*, 2013) or "hotter droughts" (Allen *et al.*, 2015; Buras *et al.*, 2020; Schuldt *et al.*, 2020). They are of particular interest due to their aggravated impacts, for example, on vegetation vitality and mortality, in comparison to drought events under "normal" climate conditions.

Different approaches and indices are used to evaluate the intensity, frequency, and duration of drought conditions and heavy precipitation events. Widely used drought indices often address monthly, seasonal, and annual time scales, like the standardized precipitation index (SPI; McKee *et al.*, 1993) and the standardized precipitation evaporation index (SPEI; Vicente-Serrano *et al.*, 2010). Many heavy precipitation indices and some dry period indices as defined by WMO (2009) are calculated based on daily data.

With regard to drought events, Spinoni *et al.* (2015b) provide an overview of the biggest events in Europe for 1950–2012 by combing three drought indices (SPI, SPEI, and reconnaissance drought index [RDI]; Tsakiris and Vangelis, 2005) at the 3-month scale for meteorological drought and the 12-month scale for hydrological drought. They also provide an extensive list of relevant references for the most important events. Their analysis identified pan-European drought events in 1950–1952, 1953–1954, 1972–1974, and 2003.

At the European scale, several drought studies based on instrumental records have shown drying trends in southern Europe, particularly in the Mediterranean region and wetting trends in northern and northeastern Europe (e.g., Briffa *et al.*, 2009; Gudmundsson and Seneviratne, 2015; Spinoni *et al.*, 2017; Stagge *et al.*, 2017). Drought trends for central Europe are spatially and seasonally more diverse and often linked to temperature increases (Spinoni *et al.*, 2015a; Hänsel *et al.*, 2019). Rising average temperatures since the 1990s increasingly impact the observed severity of drought events, especially during the warm part of the year and in southern Europe (Vicente-Serrano *et al.*, 2014; García-Herrera *et al.*, 2019).

A review by Madsen *et al.* (2014) that encompasses 46 studies with observation-based trend analyses and 33 studies relying on climate change projections for extreme precipitation and streamflow concludes that observations and climate model projections show an increase in extreme precipitation in Europe. More recent continental studies on changes in heavy precipitation based on observations (Sun *et al.*, 2021) and climate models (Li *et al.*, 2021) confirm these results. Thus, the most recent IPCC report AR6 of working group 1 (Seneviratne *et al.*, 2021) concludes that there is robust evidence that the magnitude and intensity of extreme precipitation has very likely increased since the 1950s in Europe. Such increases in extreme precipitation

are observed more frequently in summer and winter than in the transitional seasons (Madsen *et al.*, 2014).

This study analyses spatial and temporal variations and trends in drought conditions and heavy precipitation events over Europe during the warmest part of the year—here called summer half year (SHY: AMJJAS – April–May–June–July–August–September)—for the period 1901–2018. Such long-term variations and trends in drought conditions and heavy precipitation trends are of relevance for a lot of economic sectors, as they are often connected with adverse effects. Adaptation options mitigating drought risks could negatively affect resilience against heavy precipitation events and vice versa. Thus, it is important to know if one should focus on one of these extremes, or if adaptation measures capable of dealing with both extremes are needed. Some analyses are also performed for the summer season (JJA – June–July–August; results mainly reported as Supporting Information). The study is based on a spatially well-distributed dataset comprising many of the longest and most reliable station time series with daily precipitation and daily extreme temperature data available in Europe. The characteristics of European record drought summers and temporal variations in drought characteristics are studied using a range of drought indices and combining them into an aggregated drought evaluation index (ADE). Furthermore, temporal variations in three heavy precipitation indices are analysed to evaluate impact relevant shifts in the climatic conditions in Europe and five subregions. In the last step, the stations with a simultaneous increase in drought and heavy precipitation conditions are highlighted.

2 | DATA AND METHODS

2.1 | Study area and data basis

We study long-term variability in summer droughts and the specifics of five record summers such as 2018 based on 63 European stations with long time series (Figure 1). Thereby, we use the same station collective and the same regional grouping as applied by Hoy *et al.* (2020) that focused on evaluating the heat conditions during the 2018 summer. Four stations were excluded; one due to missing long-term precipitation data and three other stations due to their location north of the Polar Circle, which challenges the calculation of potential evapotranspiration (PET).

Our focus on long-term station data with comparably well-documented metadata has some advantages over using gridded datasets—especially for the analysis of extreme events and the detection of climatic trends—and some disadvantages like the limited spatial coverage. Gridded data sets (both interpolated observations like EOBS and reanalyses (e.g., ERA5) are fundamental for climate change research, but for the study of long-term trends they have significant open issues. For example, it is still an open issue how accurate reanalyses are able to estimate long term trends with confidence due to changes in global observations (Thorne and Vose, 2010; Dee *et al.*, 2011). Thus, focussing on station data adds value to grid-data-focussed studies, which typically cover shorter timescales and include inherent inhomogeneities of the used stations, which are more difficult to detect compared to using station data directly.

This study is based on station data for daily precipitation (RR), as well as daily maximum (Tx) and minimum temperature (Tn). The station datasets belong to the longest, most complete and most reliable (homogenous) time series in Europe. They have been selected to obtain a spatially well distributed dataset. This means that some nearby stations with similarly long records have not been included in the analysis in order to avoid regional imbalances in the analyses. Almost all stations are located at altitudes below 500 m (three exceptions up to 667 m). Thus, influences on the analyses by specific climatic effects from high mountain ranges are avoided.

The five regions with individual station numbers between 11 and 14 stations are

- NE (northeast; 11 stations) with a cool and rather continental climate.
- W (west; 13 stations) with a rather cool and more maritime climate.
- C (central; 14 stations) with temperate summers in the transition zone between maritime and continental climate.
- S (south; 14 stations) with subtropical summers.
- SE (southeast; 11 stations) with a warm and continental climate.

Information on the regional grouping methods, the temperature characteristics of the five regions and generally on the data basis and the quality of the station series can be obtained from Hoy *et al.* (2020). Hoy *et al.* (2020) carefully checked and described the homogeneity of the long-term temperature series that are the basis for the calculation of potential evapotranspiration, which is needed to compute some of the applied drought indices.

Our analyses start in 1901, when more than half of the stations have precipitation and temperature data available. Data availability rises during the 20th century, with some temporary drops in the availability of precipitation and temperature data towards the end of both world wars (Figure 2). Data of all stations are available

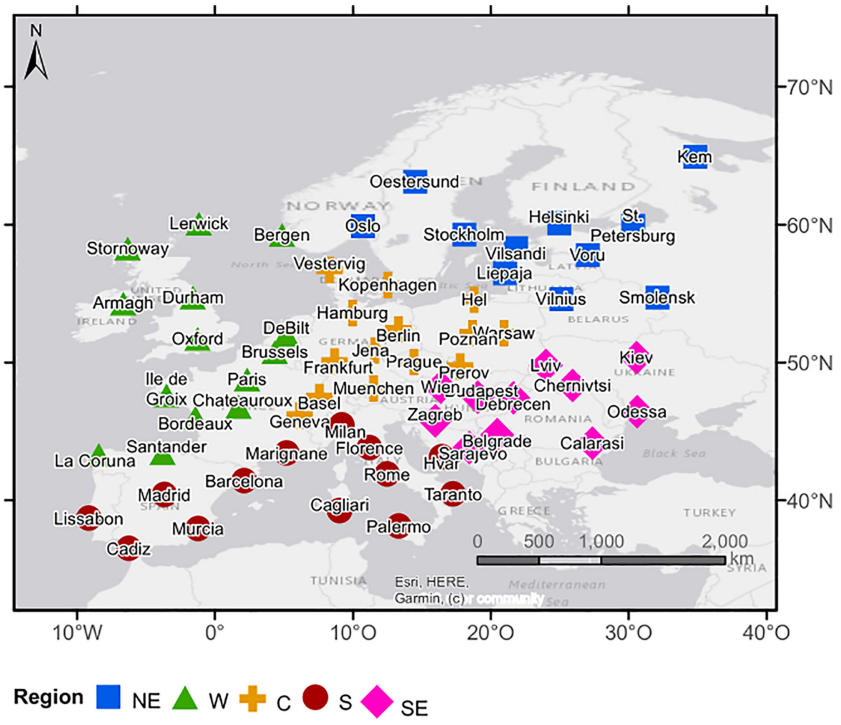

FIGURE 1 Map of the study area showing the location of the 63 meteorological stations and their classification into five subregions (NE, northeast; W, west; C, central; S, south; SE, southeast) [Colour figure can be viewed at wileyonlinelibrary.com]

since 1951, with a few exceptions during individual years. All time series are updated until October 2018 or longer. The data availability of temperature and thus potential evapotranspiration (PET) data (Figure 2b) is slightly better than that of precipitation data (Figure 2a). Thus, the availability of information on the climatic water balance (RR – PET; Figure 2c) is mainly restricted by the availability of precipitation data.

No method for filling small gaps in the daily series was applied. Our focus was on high quality and preferably complete datasets. A missing day led to the termination of a dry period that were calculated based on daily data. For the calculation of monthly precipitation and PET data, two missing days were allowed for each month. If more than 2 days in a month are missing, the monthly value is set as "not available" (na) and thus the seasonal/annual value is also set to "na."

2.2 | Climate indices

2.2.1 | Drought indices

Precipitation characteristics are evaluated using indices based on daily as well as monthly data. We are also using drought indices incorporating information on potential evapotranspiration PET as the severity of droughts may be underestimated by purely precipitation-based indices, particularly in a warming climate (Vicente-Serrano *et al.*, 2010; 2014). Our study is on meteorological drought characteristics and conclusions on soil moisture cannot be drawn directly. We are using PET and not the actual evapotranspiration in the drought index calculations. Thus, we can only compute a theoretical climatic water balance. Such a climatic water balance deviates from the actual water balance that is determining the availability of soil water for plants and the moisture fluxes to the atmosphere. Using these kind of drought indices has some limitations with respect to the evaluation of soil moisture and moisture fluxes to the atmosphere. For soils that are already depleted of moisture it does not really matter how large PET is, the actual evapotranspiration will be rather low in such cases.

Considered indices based on daily data are displayed in Table 1. Dry periods are defined as a sequence of days with precipitation below a specific threshold, whereby different studies use different thresholds like 0.1, 1.0, 5.0, and 10.0 mm·day^{-1} (Perzyna, 1994; Lana *et al.*, 2008; Cindrić *et al.*, 2010; Serra *et al.*, 2014). We use a threshold of 1.0 mm·day^{-1} for dry days (DD) that is related to evapotranspiration processes (Serra *et al.*, 2014). Additionally, a dry period definition based on the daily climatic water balance (WB) is applied. Days with a climatic water balance below zero are defined as dry days in this case. The average and maximum duration of consecutive sequences of such days are studied for both definitions. These duration indices were calculated for the entire time series first. Thereby, the duration of a dry period is assigned to the day of its end. In a second step, the results for the SHY and summer season were extracted by considering all periods whose end day lies within the respective analysis period.

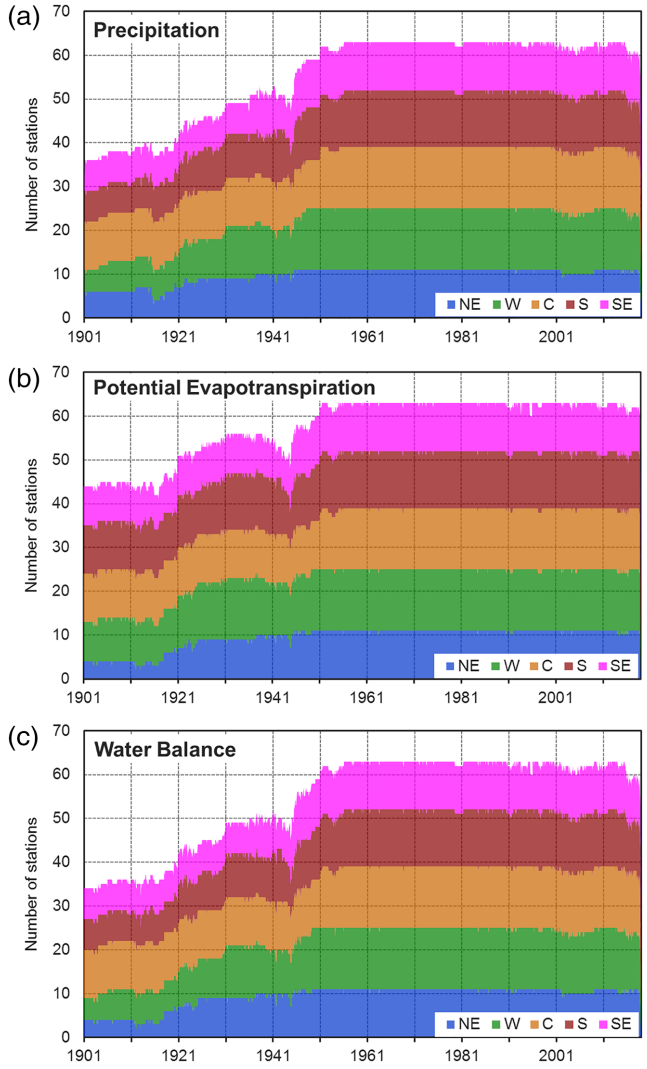

FIGURE 2 Availability of (a) precipitation and (b) potential evapotranspiration (PET) and (c) climatic water balance data at 63 stations within five subregions (NE, northeast; W, west; C, central; S: south; SE, southeast) during 1901–2018 [Colour figure can be viewed at wileyonlinelibrary.com]

On a monthly basis and for the evaluation of drought conditions on longer aggregation time scales (summer half year and summer) the rainfall anomaly index (RAI; Van Rooy, 1965) in a modified version mRAI (Hänsel *et al.*, 2016) and the water balance anomaly index (WBAI; Hänsel *et al.*, 2016) are applied (Table 1). Hoy *et al.* (2017) have shown that the mRAI delivers good comparable results to the well-known Standardized precipitation index (SPI; McKee *et al.*, 1993) over Europe, while the WBAI is comparable to the standardized precipitation evaporation index (SPEI; Vicente-Serrano *et al.*, 2010).

The indices mRAI and WBAI are calculated using a straightforward standardization approach for precipitation (RR) and the climatic water balance (WB = RR − PET),

TABLE 1 Name, definition, and units of the daily and monthly climate indices used in this study

Index	Description	Unit
DD	Number of dry days (=days with daily precipitation totals below 1 mm)	days
AvD	Average duration of dry periods (=continuous sequence of DD)	days
CDD	Consecutive dry days (maximum duration of dry periods)	days
nWBD	Number of days with a negative climatic water balance (=days with WB < 0 mm)	days
AvDnWB	Average duration of periods with days showing a negative climatic water balance	days
MxDnWB	Maximum duration of periods with days showing a negative climatic water balance	days
Rx1day	Maximum daily precipitation total	mm
R95pTOT	Precipitation fraction due to very wet days in percent (=100% * [precipitation total of days above the 95th percentile/total precipitation])	%
R99pTOT	Precipitation fraction due to extremely wet days in percent (=100% * [precipitation total of days above the 99th percentile/total precipitation])	%
mRAI	Modified rainfall anomaly index (Van Rooy, 1965; Hänsel *et al.*, 2016); anomalies of precipitation at monthly timescales	Without unit
WBAI	Water balance anomaly index (Hänsel *et al.*, 2016); anomalies of the climatic water balance (RR − PET) at monthly timescales	Without unit
ADE	Aggregated drought evaluation index (for details see section 2.2.2) Here, it integrates the information of eight standardized drought indices (mRAI, WBAI, DD, AvD, CDD, nWBD, AvDnWB, MxDnWB), but the concept can be flexibly adapted to include other indices and thus other drought characteristics	Without unit

respectively. The medians of the precipitation total and climatic water balance, respectively, are used as proxies for the average of the distribution, while the average of the 10% most extreme wet and dry cases describes the variability of the distribution. Different values representing the variability are used for each side of the distribution in order to account for skewed distributions. The mRAI of a certain month (or other aggregation period) i is calculated as follows:

$$\mathrm{mRAI}_i = \pm \mathrm{SF} * \frac{\mathrm{RR}_i - \overline{\mathrm{RR}}}{\overline{E} - \overline{\mathrm{RR}}},$$

where RR_i is the precipitation total of month i; $\overline{\mathrm{RR}}$ is the median monthly precipitation of the base period 1951–2010 for the respective month; $\overline{E}$ is the mean of the 10% most extreme precipitation totals of the base period 1951–2010 for the respective month. For negative anomalies of $\mathrm{RR}_i - \overline{\mathrm{RR}}$ the events below the 10th percentile are used and for positive anomalies those above the 90th percentile; ±SF is the scaling factor (positive for $\mathrm{RR}_i \geq \overline{\mathrm{RR}}$, and negative for $\mathrm{RR}_i < \overline{\mathrm{RR}}$).

The index is calculated using a 60-year base period, as a long base period ensures a good representation of the climate variability and the extremes of the distribution. The period 1951–2010 was chosen, as data availability is best during these 60 years allowing for a good regionally comparable derivation of the factors needed to calculate the indices.

The WBAI is calculated in the same way as illustrated for the mRAI by replacing RR with WB,

$$\mathrm{WBAI}_i = \pm \mathrm{SF} * \frac{\mathrm{WB}_i - \overline{\mathrm{WB}}}{\overline{E} - \overline{\mathrm{WB}}}.$$

Hence, the actual climatic water balance value of month i (WB_i) is compared to the median value ($\overline{\mathrm{WB}}$) of this month within 1951–2010 and the variability of the distribution is estimated by the distance of the mean of the six most extreme climatic water balance values ($\overline{E}$) to the median of the distribution. For both calculations (mRAI and WBAI) a scaling factor of SF = 1.7 is applied as suggested by Hänsel *et al.* (2016) in order to obtain similar values and class frequencies as those of SPI and SPEI. This allows using the same classification of moisture classes that were suggested by McKee *et al.* (1993) for the SPI (Table 2).

WBAI and mRAI are applied at timescales of 1, 3, and 6 months. The respective timescale is indicated by a number in the index name, for example, mRAI-6 refers to the modified rainfall anomaly index at a timescale of 6 months. The indices are used to describe the drought intensity at monthly time scale (mRAI-1 and WBAI-1), for the summer half year (mRAI-6 and WBAI-6 for September covering the entire SHY from April to September) and the summer season (mRAI-3 and WBAI-3 for August). In the following we indicate these indices without specifying the considered time scale because SHY indices are always "−6" values for September, summer indices are always "−3" values for August and monthly indices are always "−1" values referring to the considered month.

The Hargreaves–Samani approach (Hargreaves and Samani, 1985) is applied for the calculation of PET on a daily scale. It uses information on the geographical location, average precipitation totals and minimum as well as maximum daily temperatures. Thereby, minimum and maximum temperature is used to estimate solar radiation from the extraterrestrial radiation. We are using the R-package Evapotranspiration Version 1.15 with the function ET.HargreavesSamani for our calculations. The application of more complex PET calculation approaches like the Penman–Monteith formulation (Allen *et al.*, 1998) is not possible due to the restricted availability of the necessary climate parameters (e.g., relative humidity, global radiation, or wind speed). Many studies have already compared different PET parameterizations and their effect on climatic trends such as Hargreaves and Allen (2003), Vangelis *et al.* (2013), Stagge *et al.* (2014), Almorox *et al.* (2015), Mohammed and Scholz (2017), Spinoni *et al.* (2017), Zarei and Mahmoudi (2017), Moratiel *et al.* (2020), and Kaya *et al.* (2021). Several studies (Hargreaves and Allen, 2003; Mohammed and Scholz, 2017; Spinoni *et al.*, 2017) have shown that the Hargreaves–Samani approach delivers well usable results that are closer to the PET computed by the Penman–Monteith formulation than those obtained with the Thornthwaite approach (Thornthwaite, 1948). The chosen Hargreaves–Samani approach was already successfully applied in other drought trend studies over Europe

TABLE 2 Classification of the mRAI and WBAI into nine moisture classes using the same classification as suggested by McKee *et al.* (1993) for the SPI

Class	Index value	Description
1	≥2.00	Extremely wet
2	1.50–1.99	Very wet
3	1.00–1.49	Moderately wet
4	0.50–0.99	Slightly wet
5	−0.49 to 0.49	Near normal
6	−0.99 to −0.50	Slightly dry
7	−1.49 to −1.00	Moderately dry
8	−1.99 to −1.50	Severely dry
9	≤−2.00	Extremely dry

(Ionita *et al*., 2017; Spinoni *et al*., 2017; Spinoni *et al*., 2018), as was the Thornthwaite approach (Briffa *et al*., 2009; Spinoni *et al*., 2015a; 2015b). Stagge *et al*. (2014) have shown that the SPEI values are least sensitive to the chosen PET equation during the summer season, which is in the focus of this study.

2.2.2 | Standardization of indices and aggregated drought evaluation

Drought has different facets that can be measured by different indices. The Aggregated Drought Evaluation index ADE (Hänsel *et al*., 2019) is a concept that aims at integrating the information delivered by different drought indices into one evaluation, thus providing a synoptic description of many factors inducing drier conditions over Europe. It can be applied to whatever set of indices is deemed suitable to evaluate drought conditions. Here, we decided to integrate the information of eight standardized drought indices (Table 1). The ADE is derived by first standardizing the drought indices using the same approach as applied for mRAI and WBAI, so that the magnitude of the index values, their sign and the respective trends are good comparable. It is computed here by averaging mRAI, WBAI, the mean of the standardized versions of the three drought indices related to DD (DD, AvD, CDD) and the mean of the standardized versions of the three indices related to nWB (nWB, AvDnWB, MxDnWB).

2.2.3 | Heavy precipitation indices

In order to compare the observed drought trends with changes in heavy precipitation, three heavy precipitation indices are included in the analysis (see index definitions in Table 1). We use the maximum daily precipitation total per season (Rx1day) as an index for the absolute magnitude of heavy precipitation and two percentile-based indices to capture changes in the precipitation fraction on heavy precipitation days (R95pTOT, R99pTOT). The percentiles are calculated for the reference period 1961–1990.

2.3 | Methods

We decided to focus on the warm part of the year—the Northern Hemisphere summer half year (SHY; April–September). Focusing on the half years instead of the seasons helps to differentiate between a general winter (about mid-October to mid-April) and summer atmospheric circulation (mid-April to mid-October). Precipitation in the winter half year is much more dependent on the large-scale synoptic circulation than precipitation in summer half year, which is more characterized by thermal convective precipitation. Furthermore, during the SHY more frequent and severe impacts related to drought as well as heavy precipitation events are to be expected. The evolution of drought conditions often already starts in spring. Due to a soil moisture–atmosphere feedback, dry and warm conditions in spring can lead to dry and warm conditions during the summer season, even propagating further into autumn (e.g., Fischer *et al*., 2007a; 2007b).

Trend analyses were conducted for the aggregated drought evaluation index ADE and the heavy precipitation indices. Simple linear regression (least squares method) is used to identify the long-term changes within the periods 1901–2018 and 1951–2018. Trends are classified into seven categories according to trend magnitude (Table 3) for the display in trend maps. These maps illustrate the spatial consistence of trends and give information on their statistical significance. The Mann–Kendall trend test (Mann, 1945; Kendall, 1975) is used to determine the significance of trends (https://rdocumentation.org/packages/modifiedmk/versions/1.6; function: "mkttest"). Maps are additionally provided to illustrate which stations show increasing trends in drought and/or heavy precipitation. For this purpose, the stations are classified into the following four categories.

1. D: Stations showing an increase in drought conditions and negative or no trend in heavy precipitation.
2. H: Stations showing an increase in heavy precipitation events and having less severe drought conditions or showing no drought trend.
3. D + H: Stations which simultaneously show increasing drought and heavy precipitation trends.
4. N: Stations having no trend or decreasing trends in drought and/or heavy precipitation conditions.

The drought trends are determined using the ADE. An increase in drought conditions is indicated by absolute trend values <-0.25. Heavy precipitation trends are obtained by averaging the relative trends of the three heavy precipitation indices. Increasing heavy precipitation conditions are indicated by an average trend of >7% (the threshold between no trend and positive trend was 5% for R95pTOT and Rx1day, while for R99pTOT it was 10%).

No linear trends are displayed in the regionally averaged time series plots. Precipitation-based indices generally show a high temporal variability at different timescales and the computed linear trends strongly depend on the values at the beginning and the end of the time series. Therefore, 30-year averages (1901–1930, 1931–1960,

Trend category	ADE	R95pTOT, Rx1day (%)	R99pTOT (%)
Very wet	>1.0	>25	>50
Wet	0.5–1.0	15–25	30–50
Slightly wet	0.25–0.5	5–15	10–30
Indifferent	−0.25 to 0.25	−5 to 5	−10 to 10
Slightly dry	−0.5 to −0.25	−15 to −5	−30 to −10
Dry	−1.0 to −0.5	−25 to −15	−50 to −30
Very dry	<−1.0	<−25	<−50

TABLE 3 Classification of trend values used for the illustration of the spatial consistence of seasonal trends (for index abbreviations please refer to Table 1)

TABLE 4 The five most extremely dry summer half years according to the aggregated drought evaluation index (ADE) are displayed for the entire study area and its five subregions [Colour figure can be viewed at wileyonlinelibrary.com]

	Europe		West		Northeast		Southeast		Central		South	
Rank	ADE	Year	ADE	Year	ADE	Year	ADE	Year	ADE	Year	ADE	Year
1	−0.97	1947	−1.57	1921	−1.37	1901	−1.75	1946	−1.71	2018	−1.54	1945
2	−0.83	2018	−1.20	1911	−1.27	2002	−1.29	1950	−1.71	1947	−0.88	1927
3	−0.70	2003	−1.18	1976	−1.17	1959	−1.19	2015	−1.57	1976	−0.85	1922
4	−0.69	1921	−1.03	1949	−1.05	1939	−1.12	1947	−1.50	1911	−0.79	1943
5	−0.65	1911	−0.93	1955	−0.95	1941	−1.07	2009	−1.27	1921	−0.74	2017

Note: The five most extreme years over Europe are highlighted by different background colours (blue indicates years at the beginning of the 20th century, green indicates years in the middle of the 20th century, and orange/red is used to highlight years at the beginning of the 20th century). If these years also belong to the TOP5 in the five subregions, then they are highlighted by the same colour in the respective row of the subregion.

1961–1990, and 1991–2018) are used in the graphics of individual indices to indicate long-term deviations and changes. Information on the statistical significance of the linear trends is not shown, as the focus is on the long-term temporal variability of precipitation characteristics and linear trends describe those variations insufficiently.

For the display of average index information for Europe and its subregions in the time series plots a simple averaging procedure is applied on the station values. Subregional results are displayed by different symbols in addition to the average of the entire dataset. The symbols and colours are consistently used within all maps and figures in order to facilitate the identification of subregional specifics. Scatterplots and correlation analysis (Pearson-product–moment correlation) are used in order to compare the characteristics of different drought indices.

3 | RESULTS

3.1 | Summers with the most extreme drought in Europe

Based on the aggregated drought evaluation (ADE), the most extreme dry summer half years (SHY; April–September) have been identified for the study area and its five subregions (Table 4). The driest SHY occurred in 1947 (see also Figure 3 for selected individual drought indices), with dry conditions from April to October (see Figure 4). This SHY is also in the TOP5 of the central (C) and southeast (SE) regions. The second driest SHY over Europe is 2018, which is the driest SHY in region C (also refer to Figure 3 for some individual drought indices). The SHY of 2003 is ranked third, while the SHYs of 1921 and 1911 are at rank four and five. 1911 and 1921 are also in the TOP5 of the west (W) and C regions, while 2003 misses the TOP5 in each of the subregions (rank 7 in the regions W, C, south – S, and SE). The strongest similarities between the subregional TOP5 and the overall TOP5 is visible for the Central region. This is probably connected to the comparatively small distance of the region C to all other regions and the location of the centres of individual drought events. Drought events centred over one of the NE (northeast), W, S, and SE regions are more frequently related with drought conditions in the central region C than, for example, drought conditions in the northern regions with those in the southern part of Europe. High ADE-values for Europe are reached if the central region and parts of neighbouring regions are impacted, while the rest of the regions shows close to normal conditions. In contrast, a drought centre over the north or south of Europe is often connected with reverse moisture conditions in the rest of Europe and thus

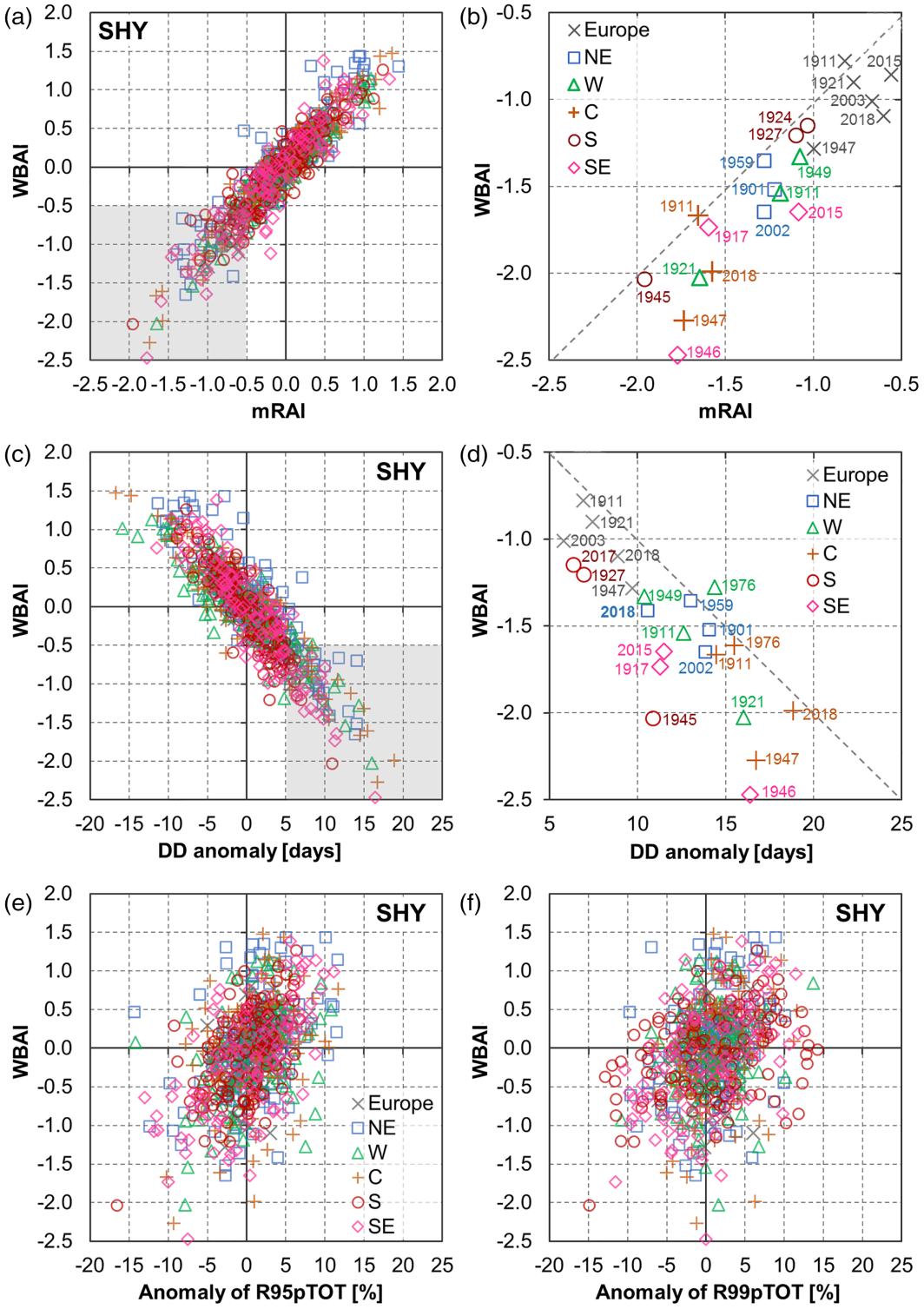

FIGURE 3 Scatterplots of regionally averaged summer half year values of (a, b) WBAI versus RAI, (c, d) WBAI versus the anomaly of dry days as well as WBAI versus (e) the anomaly of R95pTOT and (f) the anomaly of R99pTOT. Subplots (a, c, e, f) display the values of all summer half years of period 1901–2018, while subplots (b, d) present the section of the most extreme drought SHYs (TOP5 for Europe and TOP3 for the subregions; more than three subregional values may be displayed in case the TOP3 of the two displayed indices do not cover the same 3 years) [Colour figure can be viewed at wileyonlinelibrary.com]

lower overall ADE-values. Corresponding results for summer (June–August) are presented and discussed in Table S1, Supporting Information.

The comparison of the drought year rankings for the individual indices results shows some deviations, but the general identification of summers with extreme drought

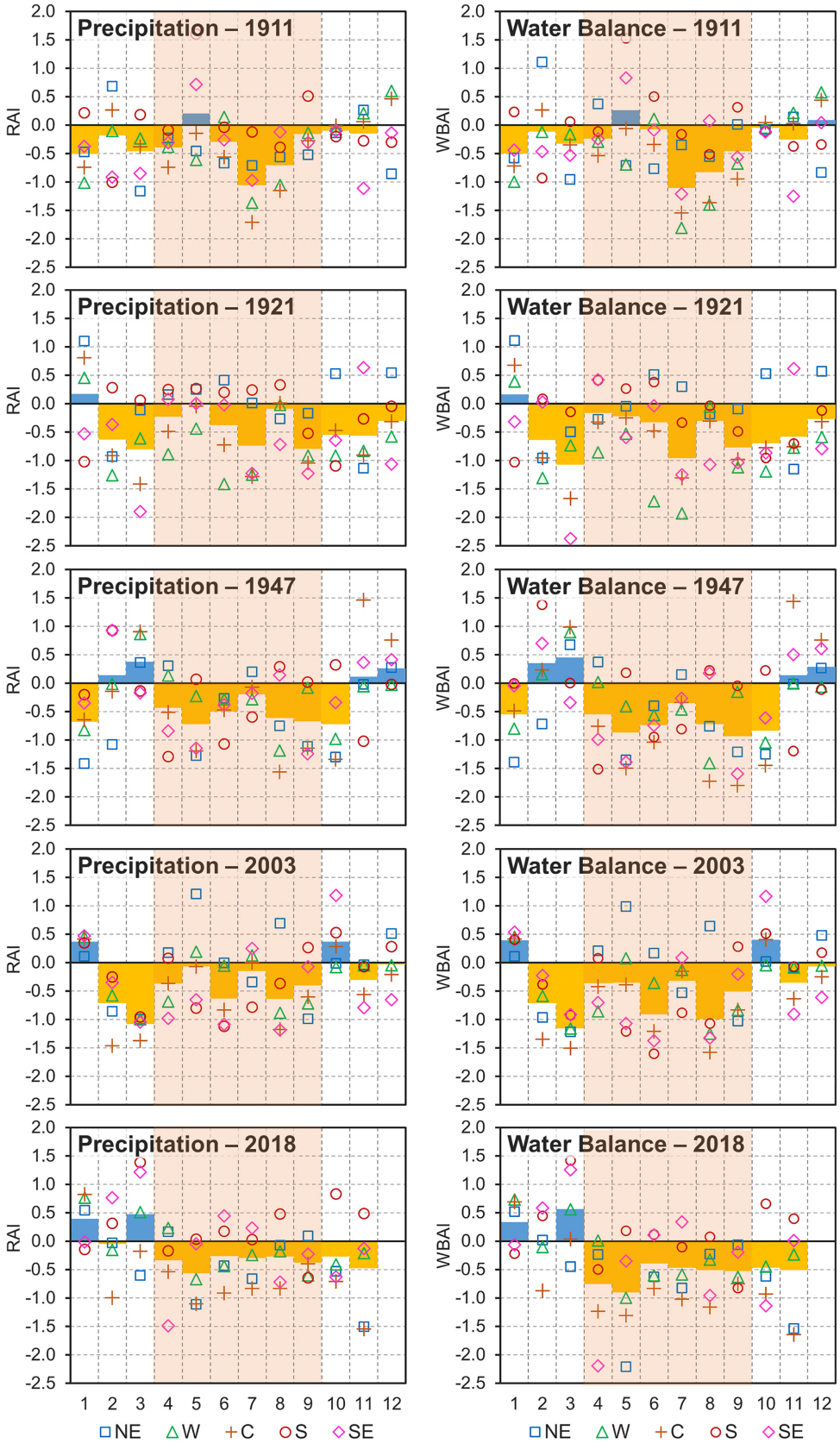

FIGURE 4 Monthly anomalies of precipitation (left) and climatic water balance (right) for the months January–December (November for 2018). Displayed are the regionally averaged anomalies for the five driest summer half years 1911, 1921, 1947, 2003, and 2018 for entire Europe (columns) as well as the five subregions (individual symbols) [Colour figure can be viewed at wileyonlinelibrary.com]

is similar. There is quite a good correlation of the purely precipitation based index mRAI and the WB-based index WBAI (Figure 3a and Table 5), as well as between the WBAI and the number of dry days (Figure 3c and Table 5). Focusing on the most extremely dry SHYs shows that there is a tendency of lower index values for

TABLE 5 Correlation matrix illustrating the correlation between different drought and heavy precipitation indices for the SHY within period 1901–1990 (upper right corner) and during the last 28 years 1991–2018 (lower left corner). Orange background colours indicate positive correlations, while blue background colours illustrate negative correlations [Colour table can be viewed at wileyonlinelibrary.com]

		1901–1990											
		ADE	**mRAI**	**WBAI**	**DD**	**AvD**	**MxD**	**WBD**	**WB-AvD**	**WB-MxD**	**R95pTOT**	**R99pTOT**	**Rx1day**
1991–2018	ADE		0.95	0.96	−0.95	−0.44	−0.39	−0.95	−0.66	−0.60	0.41	0.27	0.36
	mRAI	0.95		0.95	−0.90	−0.42	−0.27	−0.93	−0.65	−0.50	0.6	0.43	0.53
	WBAI	0.96	0.92		−0.90	−0.47	−0.30	−0.91	−0.71	−0.55	0.5	0.34	0.43
	DD	−0.92	−0.85	−0.86		0.39	0.27	0.95	0.59	0.47	−0.23	−0.10	−0.24
	AvD	−0.56	−0.57	−0.59	0.52		0.38	0.34	0.79	0.43	−0.19	0.01	−0.07
	MxD	−0.41	−0.25	−0.28	0.28	0.36		0.25	0.25	0.75	−0.13	−0.11	−0.11
	WBD	−0.95	−0.93	−0.89	0.93	0.44	0.28		0.57	0.45	−0.35	−0.20	−0.33
	WB-AvD	−0.55	−0.58	−0.56	0.48	0.76	0.14	0.46		0.51	−0.36	−0.17	−0.22
	WB-MxD	−0.45	−0.36	−0.37	0.28	0.44	0.78	0.32	0.39		−0.28	−0.19	−0.25
	R95pTOT	0.27	0.50	0.37	−0.04	−0.21	0.14	−0.25	−0.34	−0.09		0.75	0.7
	R99pTOT	0.01	0.21	0.07	0.20	−0.34	−0.10	0.05	−0.35	−0.24	0.71		0.81
	Rx1day	0.37	0.52	0.40	−0.20	−0.47	−0.16	−0.31	−0.46	−0.19	0.64	0.71	

the WBAI in comparison to the mRAI (Figure 3b). High temperatures and thus high evapotranspiration rates may significantly enhance already existing drought conditions due to a deficit in rainfall.

As all drought indices are describing different facets of the same phenomenon, they are not statistically independent. We present here the correlations between different indices to illustrate that some indices contribute more to the final ADE than others. Thereby, the ADE does not replace the use and interpretation of individual drought indices and thus specific drought characteristics. It simply supplements such individual analyses and tries to present an integrated evaluation.

The correlation matrix (Table 5) of all drought indices contributing to the definition of ADE shows very high correlation values between mRAI, WBAI, and the simple counting indices DD and nWB, while the correlation to indices measuring the duration of dry periods and periods with a negative climatic water balance is considerably lower. Negative correlations between mRAI/WBAI and the dry and negative climatic water balance periods are due to the individual index definitions, with negative values indicating drought conditions for mRAI/WBAI and positive anomalies indicating drier than normal conditions for DD and nWB and their derivatives. Comparing the correlations for periods 1901–1990 and 1991–2018 shows that the correlations between the individual drought indices are quite independent from the considered study period. The correlations between drought and heavy precipitation indices seem to depend a bit more on the chosen study period. In any case, dry SHYs are connected with lower values in the heavy precipitation indices, but the correlations between the drought indices mRAI and WBAI and the heavy precipitation indices R95pTOT and particularly R99pTOT decrease slightly during 1991–2018 in comparison to 1901–1990. This decrease is not present for Rx1day, however. The rather low correlations between the heavy precipitation indices and the drought indices based on daily data highlight that the frequency of heavy precipitation events is not strongly related to the frequency of dry and wet days.

The rainfall and climatic water balance anomalies of individual months can explain the differences in the TOP5 for the SHY and the summer season (Table S1). Figure 4 shows the mRAI and WBAI from January to December for the TOP5 SHY droughts presented in Table 4.

The monthly negative anomalies of the climatic water balance during the SHY are considerably higher (in absolute values) compared to the rainfall anomalies, particularly for the more recent years 2003 and 2018, but also for 1947. High temperatures during these years aggravated the drought

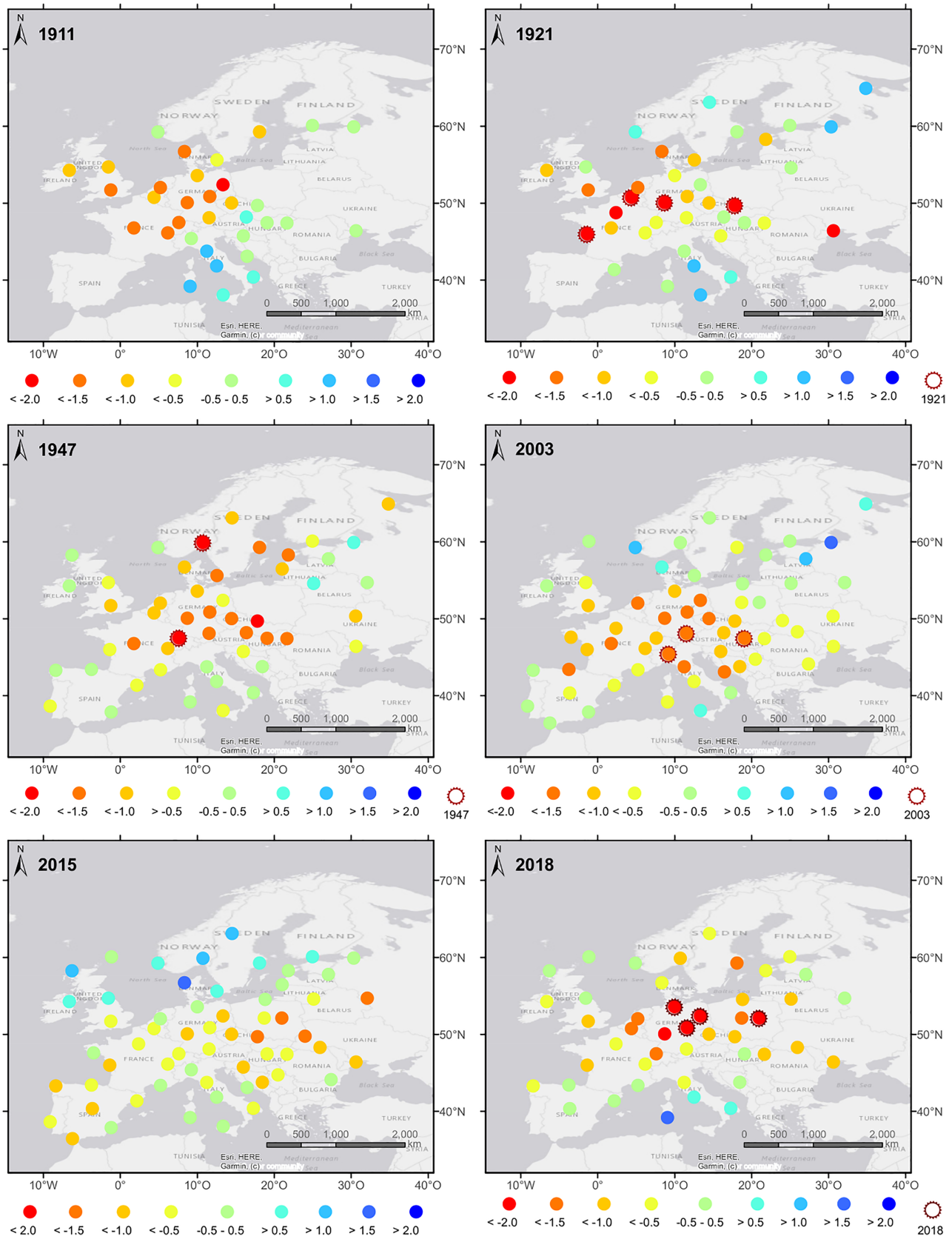

FIGURE 5 Maps of the station ADE-values for the summer half year (from extremely dry conditions in red over normal conditions in green to extremely wet conditions in blue). Displayed are the values for the five driest SHYs and additionally 2015, as an example for another recent drought summer. The sun-symbols indicate the stations that reached record values during the displayed year [Colour figure can be viewed at wileyonlinelibrary.com]

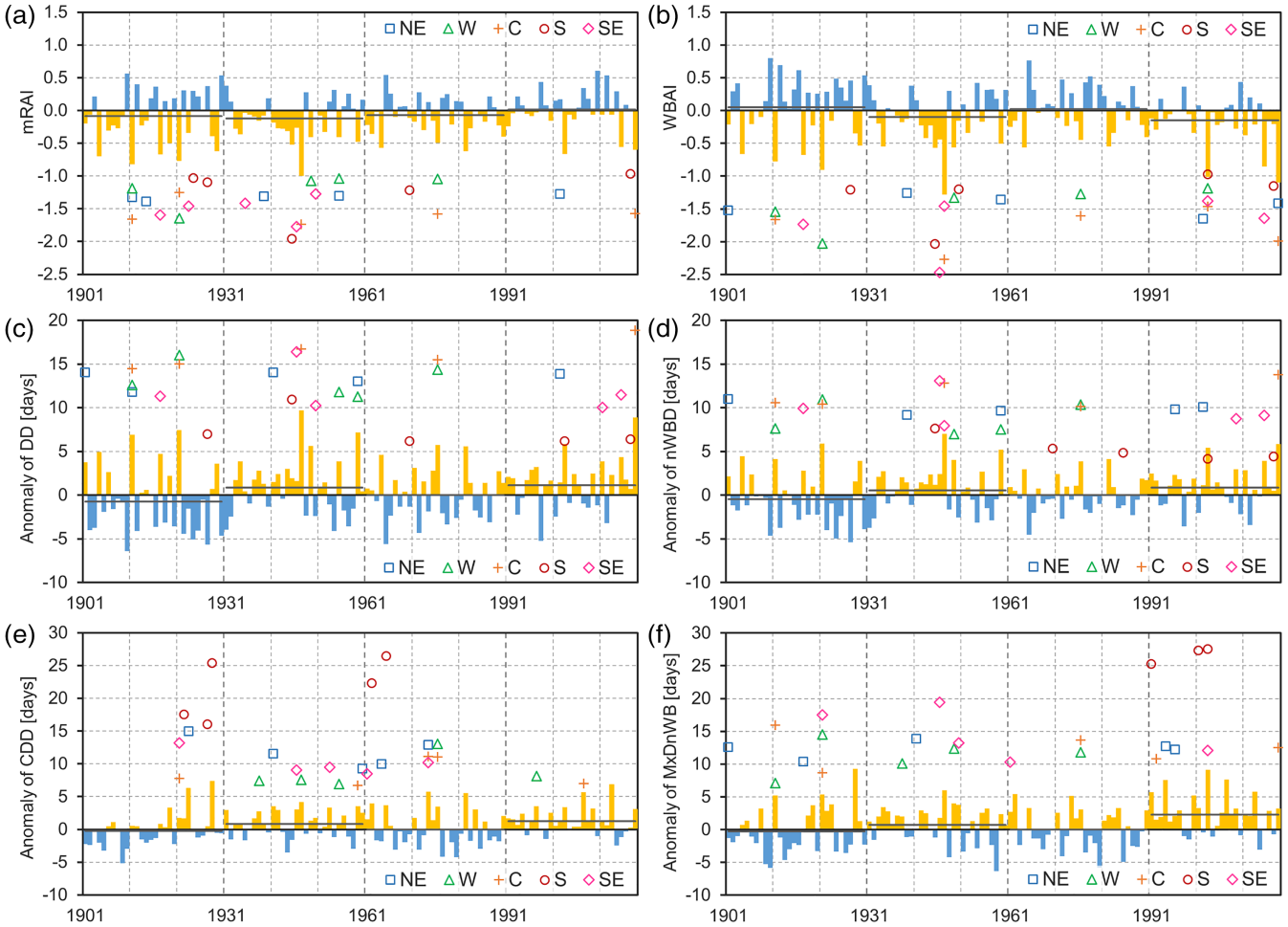

FIGURE 6 Regionally averaged SHY time series of the indices (a) mRAI, (b) WBAI, as well as the anomalies of (c) DD, (d) nWBD, (e) CDD, and (f) MxDnWB (for index definitions please refer to Table 1). Additionally, displayed are the five most extreme drought events for the five subregions [Colour figure can be viewed at wileyonlinelibrary.com]

conditions caused by rainfall deficits. The moisture preconditions before the start of the analysed SHY can significantly mitigate or aggravate the manifold drought impacts in different sectors during the successive summer months. For instance, the extensive agricultural and hydrological drought impacts in 1947 and 2018 could have been even worse without the comparatively wet March.

In addition, the of the subregional anomalies of precipitation (mRAI) and climatic water balance (WBAI) in Figure 4 illustrates that during most months and years there is quite a large variability of drought conditions over Europe. For instance, the SHY of 1921 was almost normal in the south and northwest regions, while high negative anomalies occurred in the central and west regions. Nonetheless, there are some months that have been considerably dry within all subregions; namely July 1911, June 1947 as well as February and March 2003.

The regional characteristics of the five driest years are illustrated in maps, showing the ADE value for the respective SHY (Figure 5). Additionally, the ADE of the recent extremely dry summer 2015 (rank 9 of the driest SHYs in Europe) is depicted. The SHY of 1911 has been dry in western and central Europe, while it was a normal to wet year in the south and east. This map also shows that during the first decades of the 20th century there are some restrictions in the regional coverage, as no station from the Iberian Peninsula could be included in the evaluation.

The SHY of 1921 was particularly dry around 50° northern latitude from the west to the east of the study area (Figure 5). Stations in the north as well as in the south show wet anomalies. In 1947 and 2003 the drought conditions during the SHY were very spatially extensive, covering large parts of the study area with only a few stations showing wetter than normal conditions. The drought centre in 1947 was shifted a bit more to the north as compared to 2003, where normal to wet conditions were observed at the stations in the north region.

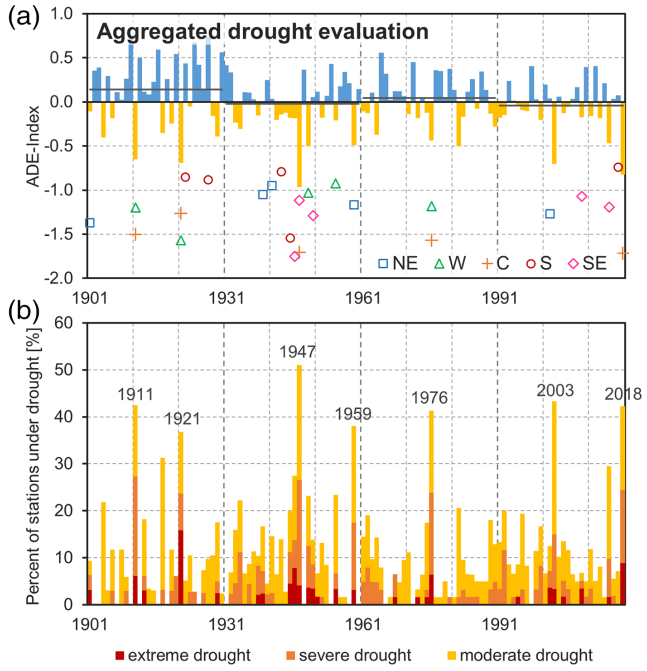

FIGURE 7 Time series of (a) the regionally averaged ADE-values for the SHY (for index definition please refer to Table 1), and (b) the percentage of stations under drought conditions according to the ADE (ADE ≤−2.0/−1.5/−1.0 for extreme/severe/moderate drought). Additionally, the five most extreme drought events for the five subregions (individual symbols) are displayed are in subplot (a) [Colour figure can be viewed at wileyonlinelibrary.com]

The drought conditions of the SHY 2015 stretched from the Iberian Peninsula and over France and Germany to the very east of the study area, while the north of Europe was wetter than normal. Very intense drought conditions during the SHY occurred in 2018 over Germany. The spatial extent of the 2018 drought is similar to the one of 1947, with drought conditions reaching north up to Scandinavia.

3.2 | Temporal changes in drought and heavy precipitation over Europe and its subregions

3.2.1 | Variations in drought characteristics

Temporal variations in the drought characteristics over Europe and its subregions are studied for several drought indices for the summer half year as well as the summer season. The time series plots show that with respect to rainfall and climatic water balance anomalies, the 1930s and in particular the 1940s have been characterized by series of dry summer half years and summers in Europe (Figure 6 and Figure S1). The last 28 SHYs and summers (1991–2018) have been on average the driest with respect to the WBAI, as compared to the three preceding 30-year averages (1901–1930, 1931–1960, and 1961–1990). With

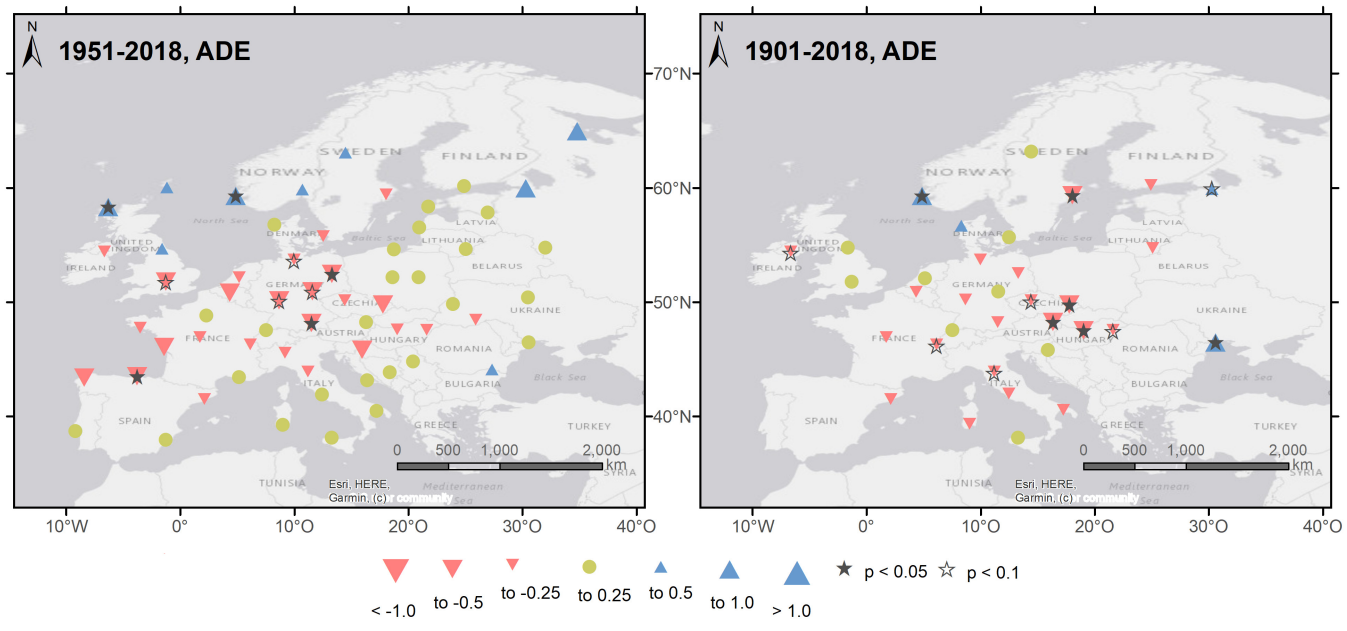

FIGURE 8 SHY trend maps showing the linear trends of ADE for the study periods 1951–2015 (left panel) and 1901–2018 (right panel). The stars indicate the statistical significance of trends according to the Mann–Kendall test [Colour figure can be viewed at wileyonlinelibrary.com]

respect to the rainfall anomalies (mRAI), the last 28-year summer and SHYs were quite close to normal conditions, with some very dry and some very wet years. This shows the strong influence of rising summer temperatures on drought conditions over Europe. The number of dry days (DD) as well as days with a negative climatic water balance (nWBD) show considerable variations, but no clear trend over the entire study area for the summer season (Figure S1). However, the number of such days increased during the SHY, suggesting that considerable increases in DD and nWBD occurred during the transition months April, May and September. A high number of DD and nWBD is potentially connected with longer consecutive sequences of dry conditions. Thus, the indices CCD and MxDnWB also reach their highest 30-year averages for the SHY during the last of the four periods, with only few small negative anomalies (Figure 6).

The ADE index time series plot (Figures 7a and S2) shows the ability of this index in capturing the main features of the individual drought indices over Europe. During the first 30-year period (1901–1930) European ADE showed positive anomalies, meaning wetter than normal conditions. The European ADE average was then very close to zero in the following 30-year period and slightly positive in the following one. Finally, European ADE reached the lowest average in the last period (1991–2018), highlighting the dry character of this period as already evident from Figure 6.

Figure 7b illustrates the spatial extent of drought conditions by plotting the fraction of stations experiencing moderate drought (ADE ≤ -1.0), severe drought (ADE ≤ -1.5) and extreme drought (ADE ≤ -2.0) conditions. Seven SHYs stand out with more than a third of the stations affected by drought conditions—these are 1947, 2003, 1911, 2018, 1976, 1959, and 1921 (in descending order). About half of the stations were under drought conditions during the SHY of 1947. The largest proportion of stations under extreme drought conditions was reached in 1921, with about 15% of the stations.

ADE index trends at individual stations are shown in Figure 8 (see Figure S3 for summer). We classify the trend magnitude into seven classes as defined in Table 3, with three classes each representing a trend towards drier (red downward triangles) and wetter (blue upward triangles) conditions, respectively, and one class (green circles) comprising low trend values and thus "no change." Additionally, the statistical significance of trends based on the Mann–Kendall test is indicated by the star symbols. Considerably less stations trends were computed for period 1901–2018 in comparison to period 1951–2018, due to the limited data availability at the beginning of the 20th century. Nonetheless, the general trend picture is quite independent from the study period. Trends towards drier conditions prevail in southern and central Europe up to a latitude of about 55°N, while several stations in the northern part of Europe show trends towards wetter SHYs. The trend category representing strong wetting or drying trend, respectively, is not reached for the ADE at station level.

3.2.2 | Changes in heavy precipitation

Temporal variations in three selected heavy precipitation indices are studied in addition to the already presented drought indices. All three indices (R95pTOT, R99pTOT, and Rx1day) show increases with respect to 30-year averages (Figure 9). The highest 30-year average over all stations is reached at the end of the study period, with almost all SHYs showing positive anomalies within 1991–2018. The SHY with by far the strongest positive anomalies of R95pTOT and R99pTOT was 2010.

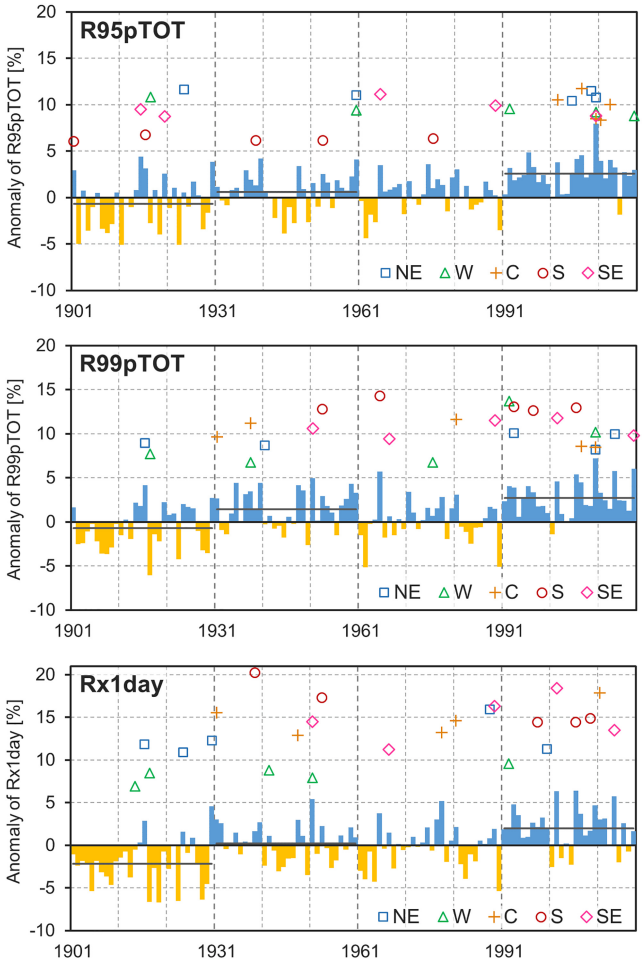

FIGURE 9 Regionally averaged SHY time series of three heavy precipitation indices, namely R95pTOT, R99pTOT, and Rx1day (for index definitions please refer to Table 1). Additionally displayed are the five most extreme SHYs with regard to heavy precipitation events for the five subregions (individual symbols) [Colour figure can be viewed at wileyonlinelibrary.com]

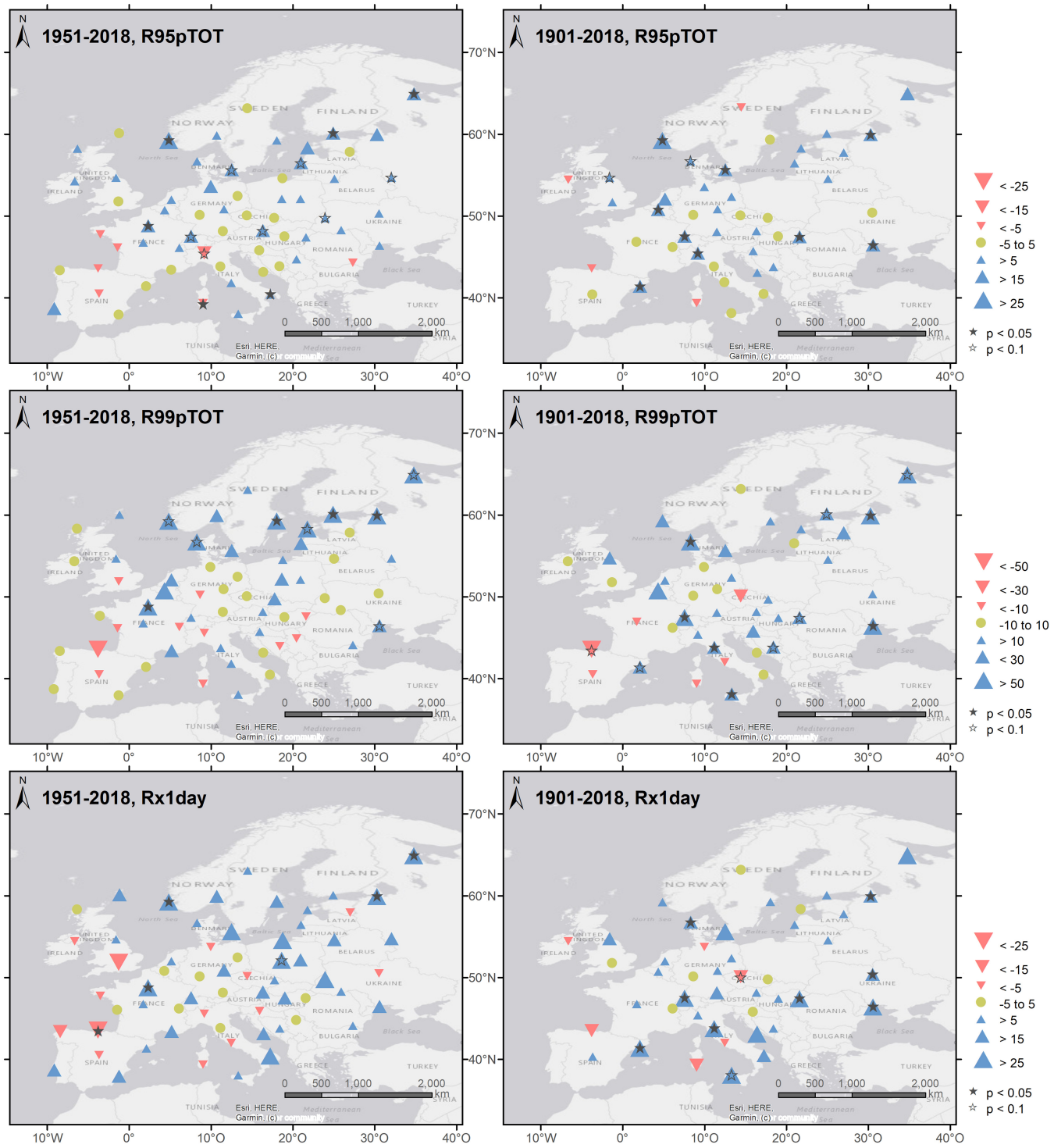

FIGURE 10 SHY trend maps showing the linear trends of three heavy precipitation indices (see Table 1 for index definitions) for the study periods 1951–2015 (left panel) and 1901–2018 (right panel). The stars indicate statistically significant trends according to the Mann–Kendall test [Colour figure can be viewed at wileyonlinelibrary.com]

The highest daily precipitation maxima (Rx1day) on average were reached during the SHYs of 2006 and 2002. The comparison with Figure 7 provides evidence that the three heavy precipitation indices were negative in the period 1901–1930, although the first 30-year period 1901–1930 showed wetter than normal condition (i.e., positive average ADE index). On the other hand, the negative ADE values for period 1991–2018 that point to drier than normal SHYs were connected with strongly positive anomalies of the heavy precipitation indices.

Focusing on the subregional TOP5 SHYs illustrates a strong influence of the chosen index on the timing of the five largest events, particularly between R95pTOT representing moderate extremes and the indices R99pTOT and Rx1day focusing on rarer events. Most of the TOP5 of R95pTOT in the two southern regions (S: 5/5; SE 4/5) occurred before 1990, while for the other two indices two (SE)/three (S) out of five record SHYs were observed during the most recent period 1991–2018. On the other hand, four of the TOP5 values of Rx1day for the regions NE, W, and C occurred before 1991, while for the other two indices 2–4 of the regional TOP5 values occurred in the most recent period 1991–2018.

Figure 10 presents the trend maps for the three heavy precipitation indices for the periods 1951–2018 and 1901–2018. The trends are classified into 7 categories (Table 3), as done for the ADE-maps (Figure 8). Significant trends according to the Mann–Kendall test are indicated by star-symbols. All three heavy precipitation indices show mainly increasing trends at the station level and just a few decreasing trends. There are more significant positive trends than one would expect to occur by chance. Larger trend values are reached for the indices addressing more extreme precipitation events (R99pTOT and Rx1day) and at the same time negative trends occur more frequently. This reflects the large natural temporal variability of heavy precipitation. Stations with positive heavy precipitation trends appear in all five subregions. There are no clear spatial differences in the trend pattern as for the drought indices.

4 | DISCUSSION

4.1 | Drought

Drought conditions during the summer season and particularly during the SHY have increased over central and southern Europe, as shown by the aggregated drought evaluation index (ADE; Figures 7 and 8). The ADE combines eight individual drought indices that are based on daily and monthly values of precipitation and climatic water balance, respectively. The ADE can also potentially integrate other drought indices, depending on the drought characteristics that are in the study focus. Comparing the different drought indices shows larger negative values—meaning drier conditions—for indices that integrate PET into their calculation, particularly during recent decades. This matches the observations of other studies (Vicente-Serrano *et al.*, 2014; Spinoni *et al.*, 2017; 2017) and it is also in good agreement with the results of Crespi *et al.* (2021) and Ranzi *et al.* (2021), that show a secular decrease (1845–2016) in runoff of the Italian river Adda by about 20%, while in the same period precipitation over the same basin decreased by only about 5%. Increasing summer temperatures are a main driver for recent drought extremes like 2003, 2015, and 2018 with the WBAI (−1.01, −0.86, and −1.10) reaching considerably lower values as compared to the mRAI (−0.67, −0.56, and −0.60). These climate change type droughts are connected with diverse negative effects on managed and natural ecosystems (Buras *et al.*, 2020). The reduced productivity reveals itself in lower agricultural yields (Bakke *et al.*, 2020) and in an increasing tree mortality (Schuldt *et al.*, 2020). In contrast, droughts at the beginning of the 20th century, for example, 1911 (mRAI: −0.82, WBAI: −0.78), are more directly connected to rainfall deficits. Nonetheless, the combination of strong rainfall deficits with high temperatures and respective impacts on atmospheric evaporative demand is nothing new to the 21st century. The summer drought of 1947 was also considerably aggravated by unusually hot temperatures (mRAI: −1.00, WBAI: −1.28). The increase in dry days as well as days with a negative climatic water balance in transition months further facilitates the development of extreme SHY drought conditions in recent and coming decades.

Several studies have put the recent drought events in a long-term perspective. Using reconstructed droughts over the last 250 years Hanel *et al.* (2018) conclude that the 2003 and 2015 droughts were the most extreme droughts driven by precipitation deficits during the vegetation periods, but their spatial extent and severity at the long-term European scale are less uncommon. The reconstruction of meteorological droughts by Cook *et al.* (2015) shows a similar or higher spatial extent for the events in 1616, 1893, and 1921 compared to recent events.

Many studies as well as the present study focus on individual drought seasons or years, but drought events may extend longer in time. The longer such a drought event persists, the more severe the negative impacts are on water availability in natural and managed systems. Thus, the studied time scale of droughts very much affects the results and conclusions, as other extreme drought events and impacts emerge if longer time scales are studied. For instance, García-Herrera *et al.* (2019) showed that the period July 2016 to June 2017 was very dry over large parts of the European continent, with widespread impacts on the water supplied, agriculture, and hydroelectric power production. The 2017 SHY and summer are not remarkably dry in our analysis, as we are not considering the moisture conditions during the winter half year. Another example is the persistence of the drought conditions of 2018 to the subsequent year 2019 (Hari *et al.*, 2020). Hari *et al.* (2020) showed that after the drought events in 2003 and 2015, vegetation health recovered and returned to its normal condition during the following years, while the impact of the 2018 drought on vegetation activities propagated to 2019. They conclude that the ongoing 2018–2019 European drought

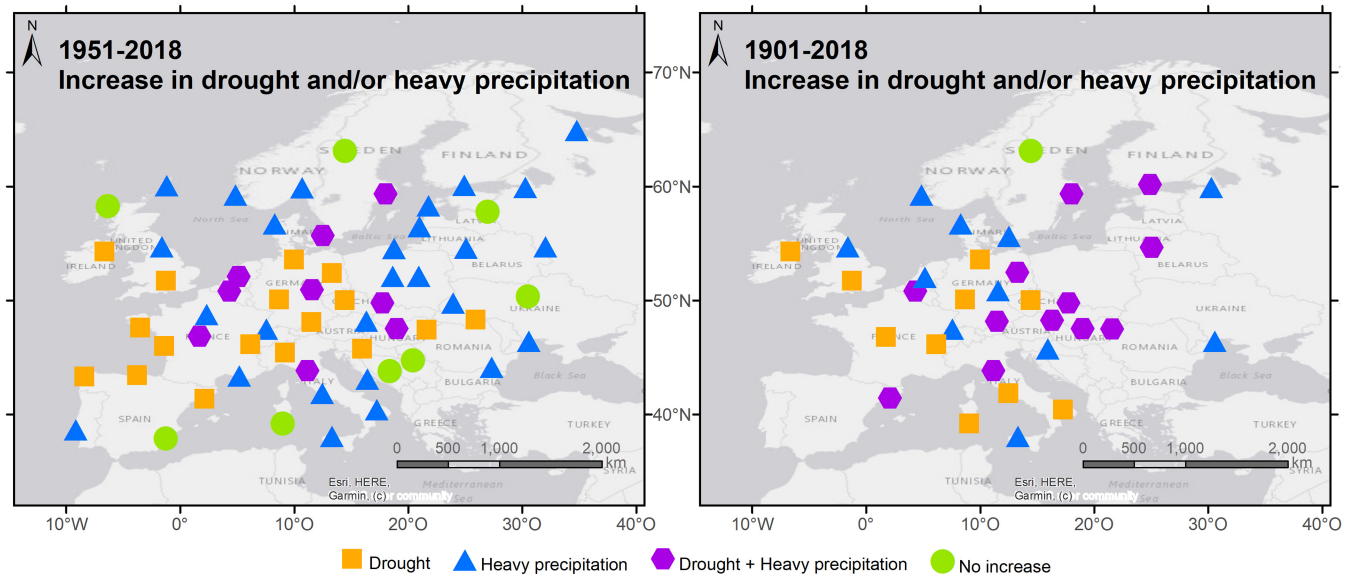

FIGURE 11 Maps categorizing the drought and heavy precipitation SHY-trends for the study periods 1951–2015 (left panel) and 1901–2018 (right panel) into four categories [Colour figure can be viewed at wileyonlinelibrary.com]

event is unprecedented in the last 250 years, with substantial implications for vegetation health. Reconstructing central European summer hydroclimate, Büntgen *et al.* (2021) found that the sequence of recent European summer droughts between 2015 and 2018 is unprecedented in the past 2,110 years within their analysed reconstructed time series. They conclude that this hydroclimatic anomaly is probably caused by anthropogenic warming and associated changes in the position of the summer jet stream. It is important to consider the different temporal scales of droughts with respect to the evaluation of the expected drought impacts during the 21st century. Hari *et al.* (2020) found a strong increase in the occurrence of such a rare event like the 2018/2019 drought in the second half of the 21st century under the RCP8.5 scenario.

Different approaches for the estimation of evapotranspiration exist. Depending on the region and season, differences occur in the evapotranspiration index numbers, which may bias the computed trends. These possible differences depend, for instance, on the ratio of the trends of average, minimum and maximum temperature. There is a need for further studies on the seasonal effects of the chosen PET parameterization approach on the drought evaluation and trends on a daily scale.

4.2 | Heavy precipitation

The investigation of three heavy precipitation indices (R95pTOT, R99pTOT, Rx1day) shows that a growing proportion of precipitation in the SHY occurs in shorter periods of time. This results in more consecutive days with less or no precipitation and therefore more severe droughts conditions, even if average precipitation amounts are unchanged in comparison to past decades. An increase in precipitation extremes at the daily scale in recent decades is support by other studies (Groisman *et al.*, 2005; Alexander *et al.*, 2006; Kunkel and Frankson, 2015; Alexander, 2016; Donat *et al.*, 2016; Fischer and Knutti, 2016). Rising global air temperatures may come along with an increasing frequency in heavy precipitation events (Allen and Ingram, 2002; Westra *et al.*, 2013; Westra *et al.*, 2014) now and in the future. This does not conflict with longer periods without or with little rain and thus increasing drought events.

The observed simultaneous increase of dry days and heavy precipitation indices during summer generally comes at the expense of moderate precipitation amounts with negative effects on soil moisture and groundwater recharge. Reduced soil moisture during the vegetation period adversely affects the productivity of terrestrial ecosystems and agricultural systems (farming and forestry) (Ruosteenoja *et al.*, 2018). Furthermore, occasional heavy precipitation falling on dry soils leads to higher surface runoff and soil erosion, with additional negative impacts on soil structure and yields.

4.3 | Drought and heavy precipitation

Drought and heavy precipitation events are both connected with specific impacts on different economic sectors and thus society. Regions that simultaneously see an increase in drought conditions and heavy precipitation events are probably exposed to higher risks and demand

broader adaptation options. Therefore, in Figure 11 we illustrate the stations which see positive drought trends (orange squares), positive heavy precipitation trends (blue triangles), and those which are exposed to both (purple hexagons). Green dots illustrate those stations that show no trends or a negative trend in one or both extreme characteristics of precipitation.

Positive drought trends are characteristic for western and central Europe, while positive heavy precipitation trends prevail in northern, central, and eastern Europe. Stations that show increasing trends in both extremes mainly occur in central Europe. The 118-year long term trends show a change signal more often than those of the shorter 68-year period 1951–2018. This illustrates the importance of analysing long, high-quality datasets that allow for a better representation of the strong natural variability of precipitation.

5 | SUMMARY AND CONCLUSIONS

The five SHYs (1947, 2018, 2003, 1921, and 1911) and summers (1911, 1904, 1983, 2003, and 1921) with record drought conditions over Europe within period 1901–2018 were studied using a station-based dataset. The 63 stations are well distributed and have high quality and long term time series of daily precipitation and daily extreme temperatures. We found trends towards drier conditions in southern and central Europe up to a latitude of about 55°N based on the ADE that integrates eight individual drought indices in our study, while several stations in the northern part of Europe show trends towards wetter SHYs and summers. The changes towards drier conditions are more pronounced for indices integrating PET into their calculation. This illustrates that the severity of summer droughts and their multiple adverse effects will increase even further within a further warming climate with related increases in the water pressure deficit, particularly over southern and central Europe.

Three heavy precipitation indices were studied in addition to the drought analyses. All three of them show the highest positive anomalies in the most recent decades (1991–2018) compared to the three preceding 30-year periods (1901–1930, 1931–1960, and 1961–1990). We see simultaneous increases in drought and heavy precipitation indices during the summer half year averaged over Europe. These simultaneous increases are characteristic for central Europe.

The recent dry summers were often connected with extremely high temperatures and heatwaves. Feedback mechanisms between drought and sensible heat fluxes from the soil may lead to a further intensification and accumulation of combined heat and drought conditions in European summers during the next decades in a progressively warming climate.

The expected continuation of the observed increasing trends in the coming decades and the manifold negative impacts connected with more intense and frequent drought, heavy precipitation and heat extremes will challenge our society and economy.

ACKNOWLEDGEMENTS

We are grateful to all dedicated people at universities, national weather services and other institutions for their priceless efforts in collecting, digitalizing, processing, and optimizing climate data. Their dedication is the basis for our study and many other climate studies. Furthermore, we acknowledge the data providers in the ECA&D project (https://www.ecad.eu). We thank Kelly Stanley for proofreading the manuscript.

AUTHOR CONTRIBUTIONS

Stephanie Hänsel: Conceptualization; data curation; formal analysis; funding acquisition; investigation; methodology; project administration; validation; visualization; writing – original draft. **Andreas Hoy:** Conceptualization; data curation; resources; writing – review and editing. **Christoph Brendel:** Formal analysis; resources; software; writing – review and editing. **Maurizio Maugeri:** Conceptualization; data curation; supervision; writing – review and editing.

ORCID

Stephanie Hänsel https://orcid.org/0000-0003-3734-0001
Andreas Hoy https://orcid.org/0000-0003-3733-6483
Maurizio Maugeri https://orcid.org/0000-0002-4110-9737

REFERENCES

Adams, H.D., Guardiola-Claramonte, M., Barron-Gafford, G.A., Villegas, J.C., Breshears, D.D., Zou, C.B., Troch, P.A. and Huxman, T.E. (2009) Temperature sensitivity of drought-induced tree mortality portends increased regional die-off under global-change-type drought. *Proceedings of the National Academy of Sciences of the United States of America*, 106, 7063–7066.

Alexander, L.V. (2016) Global observed long-term changes in temperature and precipitation extremes: a review of progress and limitations in IPCC assessments and beyond. *Weather and Climate Extremes*, 11, 4–16.

Alexander, L.V., Zhang, X., Peterson, T.C., Caesar, J., Gleason, B., Tank, A., Haylock, M., Collins, D., Trewin, B., Rahimzadeh, F., Tagipour, A., Kumar, K.R., Revadekar, J., Griffiths, G., Vincent, L., Stephenson, D.B., Burn, J., Aguilar, E., Brunet, M., Taylor, M., New, M., Zhai, P., Rusticucci, M. and Vazquez-

Aguirre, J.L. (2006) Global observed changes in daily climate extremes of temperature and precipitation. *Journal of Geophysical Research: Atmospheres*, 111, D05109.

Allen, C.D., Breshears, D.D. and McDowell, N.G. (2015) On underestimation of global vulnerability to tree mortality and forest die-off from hotter drought in the Anthropocene. *Ecosphere*, 6, 1–55.

Allen, C.D., Macalady, A.K., Chenchouni, H., Bachelet, D., McDowell, N., Vennetier, M., Kitzberger, T., Rigling, A., Breshears, D.D., Hogg, E.T., Gonzalez, P., Fensham, R., Zhang, Z., Castro, J., Demidova, N., Lim, J.-H., Allard, G., Running, S.W., Semerci, A. and Cobb, N.S. (2010) A global overview of drought and heat-induced tree mortality reveals emerging climate change risks for forests. *Forest Ecology and Management*, 259, 660–684.

Allen, M.R. and Ingram, W.J. (2002) Constraints on future changes in climate and the hydrologic cycle. *Nature*, 419, 224–232.

Allen, R.G., Pereira, L.S., Raes, D. and Smith, M. (1998) *Crop Evapotranspiration—Guidelines for Computing Crop Water Requirements. FAO Irrigation and Drainage Paper 56*. Rome: Food and Agriculture Organization of the United Nations, p. 15.

Almorox, J., Quej, V.H. and Martí, P. (2015) Global performance ranking of temperature-based approaches for evapotranspiration estimation considering Köppen climate classes. *Journal of Hydrology*, 528, 514–522.

Bakke, S.J., Ionita, M. and Tallaksen, L.M. (2020) The 2018 northern European hydrological drought and its drivers in a historical perspective. *Hydrology and Earth System Sciences*, 24, 5621–5653.

Barriopedro, D., Fischer, E.M., Luterbacher, J., Trigo, R.M. and García-Herrera, R. (2011) The hot summer of 2010: redrawing the temperature record map of Europe. *Science*, 332, 220–224.

Belz, J.-U., Adler, M., Baschek, B., Bergfeld-Wiedemann, T., Brockmann, H., Busch, N., Claes, J., Daedlow, K., Hammer, M., Hatz, M., Hillebrand, G., Hübner, G., Klein, B., Kleisinger, C., Krahe, P., Larina-Pooth, M., Meißner, D., Mothes, D., Mürlebach, M., Nilson, E., Otto, W., Promny, M., Rademacher, S., Schöl, A., Schriever, S., Schubert, B., Schwandt, D. and Viergutz, C. (2014) Das Hochwasserextrem des Jahres 2013 in Deutschland: Dokumentation und Analyse. BfG-Mitteilungen, pp. 232 Bundesanstalt für Gewässerkunde, Koblenz.

Brázdil, R., Dobrovolný, P., Bauch, M., Camenisch, C., Kiss, A., Kotyza, O., Oliński, P. and Řezníčková, L. (2020) Central Europe, 1531–1540 CE: the driest summer decade of the past five centuries? *Climate of the Past*, 16, 2125–2151.

Brazdil, R., Raska, P., Trnka, M., Zahradnicek, P., Valasek, H., Dobrovolny, P., Reznickova, L., Treml, P. and Stachon, Z. (2016) The central European drought of 1947: causes and consequences, with particular reference to the Czech lands. *Climate Research*, 70, 161–178.

Breshears, D.D., Cobb, N.S., Rich, P.M., Price, K.P., Allen, C.D., Balice, R.G., Romme, W.H., Kastens, J.H., Floyd, M.L., Belnap, J., Anderson, J.J., Myers, O.B. and Meyer, C.W. (2005) Regional vegetation die-off in response to global-change-type drought. *Proceedings of the National Academy of Sciences of the United States of America*, 102, 15144–15148.

Briffa, K., Jones, P. and Hulme, M. (1994) Summer moisture variability across Europe, 1892–1991: an analysis based on the Palmer drought severity index. *International Journal of Climatology*, 14, 475–506.

Briffa, K.R., van der Schrier, G. and Jones, P.D. (2009) Wet and dry summers in Europe since 1750: evidence of increasing drought. *International Journal of Climatology*, 29, 1894–1905.

Bronstert, A., Agarwal, A., Boessenkool, B., Crisologo, I., Fischer, M., Heistermann, M., Köhn-Reich, L., López-Tarazón, J.A., Moran, T., Ozturk, U., Reinhardt-Imjela, C. and Wendi, D. (2018) Forensic hydro-meteorological analysis of an extreme flash flood: the 2016-05-29 event in Braunsbach, SW Germany. *Science of the Total Environment*, 630, 977–991.

Bronstert, A., Agarwal, A., Boessenkool, B., Fischer, M., Heistermann, M., Köhn-Reich, L., Moran, T. and Wendi, D. (2017) Die Sturzflut von Braunsbach am 29. Mai 2016 – Entstehung, Ablauf und Schäden eines Jahrhundertereignisse. Teil 1: Meteorologische und hydrologische Analyse. *Hydrologie und Wasserbewirtschaftung*, 61, 150–162.

Büntgen, U., Urban, O., Krusic, P.J., Rybníček, M., Kolář, T., Kyncl, T., Ač, A., Koňasová, E., Čáslavský, J., Esper, J., Wagner, S., Saurer, M., Tegel, W., Dobrovolný, P., Cherubini, P., Reinig, F. and Trnka, M. (2021) Recent European drought extremes beyond common era background variability. *Nature Geoscience*, 14, 190–196.

Buras, A., Rammig, A. and Zang, C.S. (2020) Quantifying impacts of the 2018 drought on European ecosystems in comparison to 2003. *Biogeosciences*, 17, 1655–1672.

Ciais, P., Reichstein, M., Viovy, N., Granier, A., Ogée, J., Allard, V., Aubinet, M., Buchmann, N., Bernhofer, C. and Carrara, A. (2005) Europe-wide reduction in primary productivity caused by the heat and drought in 2003. *Nature*, 437, 529.

Cindrić, K., Pasarić, Z., Gajić-Čapka, M.J.T. and Climatology, A. (2010) Spatial and temporal analysis of dry spells in Croatia. *Theoretical and Applied Climatology*, 102, 171–184.

Cook, E.R., Seager, R., Kushnir, Y., Briffa, K.R., Büntgen, U., Frank, D., Krusic, P.J., Tegel, W., van der Schrier, G., Andreu-Hayles, L., Baillie, M., Baittinger, C., Bleicher, N., Bonde, N., Brown, D., Carrer, M., Cooper, R., Čufar, K., Dittmar, C., Esper, J., Griggs, C., Gunnarson, B., Günther, B., Gutierrez, E., Haneca, K., Helama, S., Herzig, F., Heussner, K.-U., Hofmann, J., Janda, P., Kontic, R., Köse, N., Kyncl, T., Levanič, T., Linderholm, H., Manning, S., Melvin, T.M., Miles, D., Neuwirth, B., Nicolussi, K., Nola, P., Panayotov, M., Popa, I., Rothe, A., Seftigen, K., Seim, A., Svarva, H., Svoboda, M., Thun, T., Timonen, M., Touchan, R., Trotsiuk, V., Trouet, V., Walder, F., Ważny, T., Wilson, R. and Zang, C. (2015) Old World megadroughts and pluvials during the common era. *Science Advances*, 1, e1500561.

Crespi, A., Brunetti, M., Ranzi, R., Tomirotti, M. and Maugeri, M. (2021) A multi-century meteo-hydrological analysis for the Adda river basin (Central Alps). Part I: gridded monthly precipitation (1800–2016) records. *International Journal of Climatology*, 41, 162–180.

De Bono, A., Peduzzi, P., Kluser, S. & Giuliani, G. (2004) Impacts of summer 2003 heat wave in Europe.

Dee, D.P., Uppala, S.M., Simmons, A.J., Berrisford, P., Poli, P., Kobayashi, S., Andrae, U., Balmaseda, M.A., Balsamo, G.,

Bauer, P., Bechtold, P., Beljaars, A.C.M., van de Berg, L., Bidlot, J., Bormann, N., Delsol, C., Dragani, R., Fuentes, M., Geer, A.J., Haimberger, L., Healy, S.B., Hersbach, H., Hólm, E. V., Isaksen, L., Kållberg, P., Köhler, M., Matricardi, M., McNally, A.P., Monge-Sanz, B.M., Morcrette, J.-J., Park, B.-K., Peubey, C., de Rosnay, P., Tavolato, C., Thépaut, J.-N. and Vitart, F. (2011) The ERA-Interim reanalysis: configuration and performance of the data assimilation system. *Quarterly Journal of the Royal Meteorological Society*, 137, 553–597.

Donat, M.G., Lowry, A.L., Alexander, L.V., O'Gorman, P.A. and Maher, N. (2016) More extreme precipitation in the world's dry and wet regions. *Nature Climate Change*, 6, 508–513.

Eamus, D., Boulain, N., Cleverly, J. and Breshears, D.D. (2013) Global change-type drought-induced tree mortality: vapor pressure deficit is more important than temperature per se in causing decline in tree health. *Ecology and Evolution*, 3, 2711–2729.

Fink, A.H., Brücher, T., Krüger, A., Leckebusch, G.C., Pinto, J.G. and Ulbrich, U. (2004) The 2003 European summer heatwaves and drought–synoptic diagnosis and impacts. *Weather*, 59, 209–216.

Fischer, E.M. and Knutti, R. (2016) Observed heavy precipitation increase confirms theory and early models. *Nature Climate Change*, 6, 986–991.

Fischer, E.M., Seneviratne, S.I., Luthi, D. and Schar, C. (2007a) Contribution of land–atmosphere coupling to recent European summer heat waves. *Geophysical Research Letters*, 34, L06707.

Fischer, E.M., Seneviratne, S.I., Vidale, P.L., Luthi, D. and Schar, C. (2007b) Soil moisture–atmosphere interactions during the 2003 European summer heat wave. *Journal of Climate*, 20, 5081–5099.

García-Herrera, R., Garrido-Perez, J.M., Barriopedro, D., Ordóñez, C., Vicente-Serrano, S.M., Nieto, R., Gimeno, L., Sorí, R. and Yiou, P. (2019) The European 2016/17 drought. *Journal of Climate*, 32, 3169–3187.

Graczyk, D. and Kundzewicz, Z.W. (2014) Changes in thermal extremes in Poland. *Acta Geophysica*, 62, 1435–1449.

Groisman, P.Y., Knight, R.W., Easterling, D.R., Karl, T.R., Hegerl, G.C. and Razuvaev, V.A.N. (2005) Trends in intense precipitation in the climate record. *Journal of Climate*, 18, 1326–1350.

Grossiord, C., Buckley, T.N., Cernusak, L.A., Novick, K.A., Poulter, B., Siegwolf, R.T.W., Sperry, J.S. and McDowell, N.G. (2020) Plant responses to rising vapor pressure deficit. *New Phytologist*, 226, 1550–1566.

Gudmundsson, L. and Seneviratne, S.I. (2015) European drought trends. In: Cudennec, C., Eicker, A., Pilon, P., Stoffel, M., Viglione, A. and Xu, Z. (Eds.) *Extreme Hydrological Events*. Copernicus Gesellschaft Mbh: Gottingen, pp. 75–79.

Hanel, M., Rakovec, O., Markonis, Y., Máca, P., Samaniego, L., Kyselý, J. and Kumar, R. (2018) Revisiting the recent European droughts from a long-term perspective. *Scientific Reports*, 8, 9499.

Hänsel, S., Schucknecht, A. and Matschullat, J. (2016) The modified rainfall anomaly index (mRAI)—Is this an alternative to the standardised precipitation index (SPI) in evaluating future extreme precipitation characteristics? *Theoretical and Applied Climatology*, 123, 827–844.

Hänsel, S., Ustrnul, Z., Łupikasza, E. and Skalak, P. (2019) Assessing seasonal drought variations and trends over central Europe. *Advances in Water Resources*, 127, 53–75.

Hargreaves, G.H. and Allen, R.G. (2003) History and evaluation of Hargreaves evapotranspiration equation. *Journal of Irrigation and Drainage Engineering*, 129, 53–63.

Hargreaves, G.H. and Samani, Z.A. (1985) Reference crop evapotranspiration from temperature. *Applied Engineering in Agriculture*, 1, 96–99.

Hari, V., Rakovec, O., Markonis, Y., Hanel, M. and Kumar, R. (2020) Increased future occurrences of the exceptional 2018–2019 central European drought under global warming. *Scientific Reports*, 10, 12207.

Hlavinka, P., Trnka, M., Semeradova, D., Dubrovský, M., Žalud, Z. and Možný, M. (2009) Effect of drought on yield variability of key crops in Czech Republic. *Agricultural and Forest Meteorology*, 149, 431–442.

Hoy, A., Hänsel, S. and Maugeri, M. (2020) An endless summer: 2018 heat episodes in Europe in the context of secular temperature variability and change. *International Journal of Climatology*, 40, 6315–6336.

Hoy, A., Hänsel, S., Skalak, P., Ustrnul, Z. and Bochníček, O. (2017) The extreme European summer of 2015 in a long-term perspective. *International Journal of Climatology*, 37, 943–962.

Hueso, S., García, C. and Hernández, T. (2012) Severe drought conditions modify the microbial community structure, size and activity in amended and unamended soils. *Soil Biology and Biochemistry*, 50, 167–173.

Ionita, M., Tallaksen, L.M., Kingston, D.G., Stagge, J.H., Laaha, G., Van Lanen, H.A.J., Scholz, P., Chelcea, S.M. and Haslinger, K. (2017) The European 2015 drought from a climatological perspective. *Hydrology and Earth System Sciences*, 21, 1397–1419.

Junghänel, T., Bissolli, P., Daßler, J., Fleckenstein, F., Imbery, F., Janssen, W., Kaspar, F., Lengfeld, K., Leppelt, T., Rauthe, M., Rauthe-Schöch, A., Rocek, M., Walawender, E. and Weigl, E. (2021) Hydro-klimatologische Einordnung der Stark- und Dauerniederschläge in Teilen Deutschlands im Zusammenhang mit dem Tiefdruckgebiet „Bernd" vom 12. bis 19. Juli 2021. pp. 16. Deutscher Wetterdienst, Offenbach.

Kaya, Y.Z., Zelenakova, M., Üneş, F., Demirci, M., Hlavata, H. and Mesaros, P. (2021) Estimation of daily evapotranspiration in Košice City (Slovakia) using several soft computing techniques. *Theoretical and Applied Climatology*, 144, 287–298.

Kendall, M. (1975) *Rank Correlation Methods*. London: Charles Griffin.

Koehler, G., Schwab, M., Finke, W. and Belz, J. (2007) An overview of the drought period 2003 in Germany: causes-impacts-consequences [Ueberblick zur Niedrigwasserperiode 2003 in Deutschland: Ursachen-Wirkungen-Folgen]. *Hydrologie und Wasserbewirtschaftung/Hydrology and Water Resources Management-Germany*, 51, 118–129.

Kohn, I., Rosin, K., Freudiger, D., Belz, J.U., Stahl, K. and Weiler, M. (2014) Niedrigwasser in Deutschland 2011. *Hydrologie und Wasserbewirtsschaftung*, 58, 4–17.

Kreienkamp, F., Philip, S.Y., Tradowsky, J.S., Kew, S.F., Lorenz, P., Arrighi, J., Belleflamme, A., Bettmann, T., Caluwaerts, S., Chan, S.C., Ciavarella, A., De Cruz, L., de Vries, H., Demuth, N., Ferrone, A., Fischer, E.M., Fowler, H.J., Goergen, K., Heinrich, D., Heinrichs, Y., Lenderink, G., Kaspar, F., Nilson, E., Otto, F.E.L., Ragone, F., Seneviratne, S. I., Singh, R.K., Skalevag, A., Termonia, P., Thalheimer, L., van

Aalst, M., Van den Bergh, J., Van de Vyver, H., Vannitsem, S., van Oldenborgh, G.J., Van Schaeybroeck, B., Vautard, R., Vonk, D. and Wanders, N. (2021) Rapid attribution of heavy rainfall events leading to the severe flooding in Western Europe during July 2021. (ed. W.W. Attribution), pp. 51.

Kundzewicz, Z.W., Ulbrich, U., Brucher, T., Graczyk, D., Kruger, A., Leckebusch, G.C., Menzel, L., Pinskwar, I., Radziejewski, M. and Szwed, M. (2005) Summer floods in central Europe: climate change track? *Natural Hazards*, 36, 165–189.

Kunkel, K.E. and Frankson, R.M. (2015) Global land surface extremes of precipitation: data limitations and trends. *Journal of Extreme Events*, 2, 1550004.

Laaha, G., Gauster, T., Tallaksen, L.M., Vidal, J.P., Stahl, K., Prudhomme, C., Heudorfer, B., Vlnas, R., Ionita, M., Van Lanen, H.A.J., Adler, M.J., Caillouet, L., Delus, C., Fendekova, M., Gailliez, S., Hannaford, J., Kingston, D., Van Loon, A.F., Mediero, L., Osuch, M., Romanowicz, R., Sauquet, E., Stagge, J.H. and Wong, W.K. (2017) The European 2015 drought from a hydrological perspective. *Hydrology and Earth System Sciences*, 21, 3001–3024.

Lana, X., Martínez, M.D., Burgueño, A., Serra, C., Martín-Vide, J. and Gómez, L. (2008) Spatial and temporal patterns of dry spell lengths in the Iberian Peninsula for the second half of the twentieth century. *Theoretical and Applied Climatology*, 91, 99–116.

Li, C., Zwiers, F., Zhang, X., Li, G., Sun, Y. and Wehner, M. (2021) Changes in annual extremes of daily temperature and precipitation in CMIP6 models. *Journal of Climate*, 34, 3441–3460.

Lloyd-Hughes, B. and Saunders, M.A. (2002) A drought climatology for Europe. *International Journal of Climatology*, 22, 1571–1592.

Madsen, H., Lawrence, D., Lang, M., Martinkova, M. and Kjeldsen, T.R. (2014) Review of trend analysis and climate change projections of extreme precipitation and floods in Europe. *Journal of Hydrology*, 519, 3634–3650.

Mann, H.B. (1945) Nonparametric tests against trend. *Econometrica*, 13, 245–259.

Masante, D., Barbosa, P. & McCormick, N. (2018) Drought in central-northern Europe – July 2018. EDO analytical report (ed. E.D. Observatory), pp. 13. JRC European drought observatory (EDO) and ERCC analytical team.

McKee, T.B., Doesken, N.J. and Kleist, J. (1993) The relationship of drought frequency and duration to time scales. In: *Proceedings of the 8th Conference on Applied Climatology*. Boston, MA: American Meteorological Society, pp. 179–183.

Merz, B., Elmer, F., Kunz, M., Muhr, B., Schroter, K. and Uhlemann-Elmer, S. (2014) The extreme flood in June 2013 in Germany. *Houille Blanche-Revue Internationale De L Eau*, 100, 5–10.

Mohammed, R. and Scholz, M. (2017) Impact of evapotranspiration formulations at various elevations on the reconnaissance drought index. *Water Resources Management*, 31, 531–548.

Moratiel, R., Bravo, R., Saa, A., Tarquis, A.M. and Almorox, J. (2020) Estimation of evapotranspiration by the Food and Agricultural Organization of the United Nations (FAO) Penman–Monteith temperature (PMT) and Hargreaves–Samani (HS) models under temporal and spatial criteria—a case study in Duero basin (Spain). *Natural Hazards and Earth System Sciences*, 20, 859–875.

Nicholson, S.E., Tucker, C.J. and Ba, M.B. (1998) Desertification, drought, and surface vegetation: an example from the west African Sahel. *Bulletin of the American Meteorological Society*, 79, 815–830.

Perzyna, G. (1994) Spatial and temporal characteristics of maximum dry spells in southern Norway. *International Journal of Climatology*, 14, 895–909.

Peters, W., Bastos, A., Ciais, P. and Vermeulen, A. (2020) A historical, geographical and ecological perspective on the 2018 European summer drought. *Philosophical Transactions of the Royal Society B: Biological Sciences*, 375, 20190505.

Pfister, C. (2018) The "Black Swan" of 1540: aspects of a European Megadrought. In: *Climate Change and Cultural Transition in Europe*. Leiden, The Netherlands: Brill, pp. 156–194.

Piper, D., Kunz, M., Ehmele, F., Mohr, S., Muhr, B., Kron, A. and Daniell, J. (2016) Exceptional sequence of severe thunderstorms and related flash floods in May and June 2016 in Germany—part 1: meteorological background. *Natural Hazards and Earth System Sciences*, 16, 2835–2850.

Ranzi, R., Michailidi, E.M., Tomirotti, M., Crespi, A., Brunetti, M. and Maugeri, M. (2021) A multi-century meteo-hydrological analysis for the Adda river basin (Central Alps). Part II: daily runoff (1845–2016) at different scales. *International Journal of Climatology*, 41, 181–199.

Rebetez, M., Mayer, H., Dupont, O., Schindler, D., Gartner, K., Kropp, J.P. and Menzel, A. (2006) Heat and drought 2003 in Europe: a climate synthesis. *Annals of Forest Science*, 63, 569–577.

Ruosteenoja, K., Markkanen, T., Venäläinen, A., Räisänen, P. and Peltola, H. (2018) Seasonal soil moisture and drought occurrence in Europe in CMIP5 projections for the 21st century. *Climate Dynamics*, 50, 1177–1192.

Schröter, K., Kunz, M., Elmer, F., Mühr, B. and Merz, B. (2015) What made the June 2013 flood in Germany an exceptional event? A hydro-meteorological evaluation. *Hydrology and Earth System Sciences*, 19, 309–327.

Schuldt, B., Buras, A., Arend, M., Vitasse, Y., Beierkuhnlein, C., Damm, A., Gharun, M., Grams, T.E.E., Hauck, M., Hajek, P., Hartmann, H., Hiltbrunner, E., Hoch, G., Holloway-Phillips, M., Körner, C., Larysch, E., Lübbe, T., Nelson, D.B., Rammig, A., Rigling, A., Rose, L., Ruehr, N.K., Schumann, K., Weiser, F., Werner, C., Wohlgemuth, T., Zang, C.S. and Kahmen, A. (2020) A first assessment of the impact of the extreme 2018 summer drought on central European forests. *Basic and Applied Ecology*, 45, 86–103.

Sedlmeier, K., Feldmann, H. and Schadler, G. (2018) Compound summer temperature and precipitation extremes over central Europe. *Theoretical and Applied Climatology*, 131, 1493–1501.

Seneviratne, S.I., Zhang, X., Adnan, M., Badi, W., Dereczynski, C., Luca, A.D., Ghosh, S., Iskandar, I., Kossin, J., Lewis, S., Otto, F., Pinto, I., Satoh, M., Vicente-Serrano, S.M., Wehner, M. and Zhou, B. (2021) Weather and climate extreme events in a changing climate. In: Masson-Delmotte, V., Zhai, P., Pirani, A., Connors, S.L., Péan, C., Berger, S., Caud, N., Chen, Y., Goldfarb, L., Gomis, M.I., Huang, M., Leitzell, K., Lonnoy, E., Matthews, J.B.R., Maycock, T.K., Waterfield, T., Yelekçi, O., Yu, R. and Zhou, B. (Eds.) *Climate Change 2021: The Physical Science Basis. Contribution of Working Group I to the Sixth Assessment Report of the Intergovernmental Panel on Climate Change*. Cambridge University Press.

Serra, C., Martinez, M.D., Lana, X. and Burgueno, A. (2014) European dry spell regimes (1951–2000): clustering process and time trends. *Atmospheric Research*, 144, 151–174.

Socher, M. and Bohme-Korn, G. (2008) Central European floods 2002: lessons learned in Saxony. *Journal of Flood Risk Management*, 1, 123–129.

Spinoni, J., Naumann, G., Vogt, J. and Barbosa, P. (2015a) European drought climatologies and trends based on a multi-indicator approach. *Global and Planetary Change*, 127, 50–57.

Spinoni, J., Naumann, G. and Vogt, J.V. (2017) Pan-European seasonal trends and recent changes of drought frequency and severity. *Global and Planetary Change*, 148, 113–130.

Spinoni, J., Naumann, G., Vogt, J.V. and Barbosa, P. (2015b) The biggest drought events in Europe from 1950 to 2012. *Journal of Hydrology: Regional Studies*, 3, 509–524.

Spinoni, J., Vogt, J.V., Naumann, G., Barbosa, P. and Dosio, A. (2018) Will drought events become more frequent and severe in Europe? *International Journal of Climatology*, 38, 1718–1736.

Stagge, J.H., Kingston, D.G., Tallaksen, L.M. and Hannah, D.M. (2017) Observed drought indices show increasing divergence across Europe. *Scientific Reports*, 7, 10.

Stagge, J.H., Tallaksen, L.M., Xu, C.Y. and Van Lanen, H.A.J. (2014) Standardized precipitation-evapotranspiration index (SPEI): Sensitivity to potential evapotranspiration model and parameters. In: Daniell, T.M., VanLanen, H.A.J., Demuth, S., Laaha, G., Servat, E., Mahe, G., Boyer, J.F., Paturel, J.M., Dezetter, A. and Ruelland, D. (Eds.) *Hydrology in a Changing World: Environmental and Human Dimensions*, Montpellier: Copernicus GmbH, pp. 367–373.

Sun, Q., Zhang, X., Zwiers, F., Westra, S. and Alexander, L.V. (2021) A global, continental, and regional analysis of changes in extreme precipitation. *Journal of Climate*, 34, 243–258.

Thieken, A.H., Bessel, T., Kienzler, S., Kreibich, H., Muller, M., Pisi, S. and Schroter, K. (2016) The flood of June 2013 in Germany: how much do we know about its impacts? *Natural Hazards and Earth System Sciences*, 16, 1519–1540.

Thieken, A.H., Muller, M., Kreibich, H. and Merz, B. (2005) Flood damage and influencing factors: New insights from the August 2002 flood in Germany. *Water Resources Research*, 41, W12430.

Thorne, P.W. and Vose, R.S. (2010) Reanalyses suitable for characterizing long-term trends. *Bulletin of the American Meteorological Society*, 91, 353–362.

Thornthwaite, C.W. (1948) An approach toward a rational classification of climate. *Geographical Review*, 38, 55–94.

Tsakiris, G. and Vangelis, H. (2005) Establishing a drought index incorporating evapotranspiration. *European Water*, 9, 3–11.

Ulbrich, U., Brücher, T., Fink, A.H., Leckebusch, G.C., Krüger, A. and Pinto, J.G. (2003) The central European floods of August 2002: part 1–rainfall periods and flood development. *Weather*, 58, 371–377.

Van der Schrier, G., Briffa, K., Jones, P. and Osborn, T. (2006) Summer moisture variability across Europe. *Journal of Climate*, 19, 2818–2834.

Van Rooy, M. (1965) A rainfall anomaly index independent of time and space. *Notos*, 14, 6.

Vangelis, H., Tigkas, D. and Tsakiris, G. (2013) The effect of PET method on reconnaissance drought index (RDI) calculation. *Journal of Arid Environments*, 88, 130–140.

Vicente-Serrano, S.M., Beguería, S. and López-Moreno, J.I. (2010) A multiscalar drought index sensitive to global warming: the standardized precipitation evapotranspiration index. *Journal of Climate*, 23, 1696–1718.

Vicente-Serrano, S.M., Lopez-Moreno, J.I., Beguería, S., Lorenzo-Lacruz, J., Sanchez-Lorenzo, A., García-Ruiz, J.M., Azorin-Molina, C., Morán-Tejeda, E., Revuelto, J., Trigo, R., Coelho, C. and Espejo, F. (2014) Evidence of increasing drought severity caused by temperature rise in southern Europe. *Environmental Research Letters*, 9, 044001.

Wang, H.J., Sun, J.Q., Chen, H.P., Zhu, Y.L., Zhang, Y., Jiang, D.B., Lang, X.M., Fan, K., Yu, E.T. and Yang, S. (2012) Extreme climate in China: facts, simulation and projection. *Meteorologische Zeitschrift*, 21, 279–304.

Westra, S., Alexander, L.V. and Zwiers, F.W. (2013) Global increasing trends in annual maximum daily precipitation. *Journal of Climate*, 26, 3904–3918.

Westra, S., Fowler, H.J., Evans, J.P., Alexander, L.V., Berg, P., Johnson, F., Kendon, E.J., Lenderink, G. and Roberts, N.M. (2014) Future changes to the intensity and frequency of short-duration extreme rainfall. *Reviews of Geophysics*, 52, 522–555.

Wetter, O., Pfister, C., Werner, J.P., Zorita, E., Wagner, S., Seneviratne, S.I., Herget, J., Grunewald, U., Luterbacher, J., Alcoforado, M.J., Barriendos, M., Bieber, U., Brazdil, R., Burmeister, K.H., Camenisch, C., Contino, A., Dobrovolny, P., Glaser, R., Himmelsbach, I., Kiss, A., Kotyza, O., Labbe, T., Limanowka, D., Litzenburger, L., Nordli, O., Pribyl, K., Retso, D., Riemann, D., Rohr, C., Siegfried, W., Soderberg, J. and Spring, J. L. (2014) The year-long unprecedented European heat and drought of 1540-a worst case. *Climatic Change*, 125, 349–363.

WMO. (2009) Guidelines on analysis of extremes in a changing climate in support of informed decisions for adaptation. In: *Climate Data and Monitoring*. Geneva: World Meteorological Organization (WMO). WCDMP-No. 72, pp. 52.

Yuan, W., Zheng, Y., Piao, S., Ciais, P., Lombardozzi, D., Wang, Y., Ryu, Y., Chen, G., Dong, W., Hu, Z., Jain, A.K., Jiang, C., Kato, E., Li, S., Lienert, S., Liu, S., Nabel, J.E.M.S., Qin, Z., Quine, T., Sitch, S., Smith, W.K., Wang, F., Wu, C., Xiao, Z. and Yang, S. (2019) Increased atmospheric vapor pressure deficit reduces global vegetation growth. *Science Advances*, 5, eaax1396.

Zarei, A.R. and Mahmoudi, M.R. (2017) Evaluation of changes in RDIst index effected by different potential evapotranspiration calculation methods. *Water Resources Management*, 31, 4981–4999.

Zscheischler, J. and Fischer, E.M. (2020) The record-breaking compound hot and dry 2018 growing season in Germany. *Weather and Climate Extremes*, 29, 100270.

SUPPORTING INFORMATION

Additional supporting information may be found in the online version of the article at the publisher's website.

How to cite this article: Hänsel, S., Hoy, A., Brendel, C., & Maugeri, M. (2022). Record summers in Europe: Variations in drought and heavy precipitation during 1901–2018. *International Journal of Climatology*, *42*(12), 6235–6257. https://doi.org/10.1002/joc.7587